applied sciences

MDPI

Article

$^{3}He/^{4}He$ Signature of Magmatic Fluids from Telica (Nicaragua) and Baru (Panama) Volcanoes, Central American Volcanic Arc

Andrea L. Rizzo [1,2], Philippe Robidoux [3,*], Alessandro Aiuppa [4] and Andrea Di Piazza [5]

1 Istituto Nazionale di Geofisica e Vulcanologia, Sezione di Milano, Via Alfonso Corti 12, 20133 Milano, Italy; andrea.rizzo@ingv.it
2 Istituto Nazionale di Geofisica e Vulcanologia, Sezione di Palermo, Via Ugo La Malfa 153, 90146 Palermo, Italy
3 Centro de Excelencia en Geotermia de los Andes (CEGA) y Departamento de Geología, Facultad de Ciencias Físicas y Matemáticas, Universidad de Chile, Plaza Ercilla 803, Santiago 8370450, Chile
4 Dipartimento DiSTeM, Università di Palermo, Via Archirafi 36, 90123 Palermo, Italy; alessandro.aiuppa@unipa.it
5 Istituto Nazionale di Geofisica e Vulcanologia, Sezione di Roma1, Via di Vigna Murata 605, 00143 Roma, Italy; andreadipiazza@gmail.com
* Correspondence: robidouxphilippe@gmail.com; Tel.: +56-951232150

Featured Application: The use of noble gas isotopic signature of fluid inclusions is increasingly being applied as a complement to traditional volcanic gas sampling and monitoring techniques. The chemical signature of fluid inclusions trapped in minerals from volcanic rocks help in interpreting fluctuations in surface gas signature in response to changes in volcanic activity and interaction with shallow hydrothermal-crustal fluids, therefore representing an applied methodology to constrain the magmatic signature and survey volcanic hazards.

Abstract: Constraining the magmatic $^{3}He/^{4}He$ signature of fluids degassed from a magmatic system is crucial for making inferences on its mantle source. This is especially important in arc volcanism, where variations in the composition of the wedge potentially induced by slab sediment fluids must be distinguished from the effects of magma differentiation, degassing, and crustal contamination. The study of fluid inclusions (FIs) trapped in minerals of volcanic rocks is becoming an increasingly used methodology in geochemical studies that integrates the classical study of volcanic and geothermal fluids. Here, we report on the first noble gas (He, Ne, Ar) concentrations and isotopic ratios of FI in olivine (Ol) and pyroxene (Px) crystals separated from eruptive products of the Telica and Baru volcanoes, belonging to the Nicaraguan and Panamanian arc-segments of Central America Volcanic arc (CAVA). FIs from Telica yield air corrected $^{3}He/^{4}He$ (Rc/Ra) of 7.2–7.4 Ra in Ol and 6.1–7.3 in Px, while those from Baru give 7.1–8.0 Ra in Ol and 4.2–5.8 Ra in Px. After a data quality check and a comparison with previous $^{3}He/^{4}He$ measurements carried out on the same volcanoes and along CAVA, we constrained a magmatic Rc/Ra signature of 7.5 Ra for Telica and of 8.0 Ra for Baru, both within the MORB range (8 ± 1 Ra). These $^{3}He/^{4}He$ differences also reflect variations in the respective arc-segments, which cannot be explained by radiogenic ^{4}He addition due to variable crust thickness, as the mantle beneath Nicaragua and Panama is at about 35 and 30 km, respectively. We instead highlight that the lowest $^{3}He/^{4}He$ signature observed in the Nicaraguan arc segment reflects a contamination of the underlying wedge by slab sediment fluids. Rc/Ra values up to 9.0 Ra are found at Pacaya volcano in Guatemala, where the crust is 45 km thick, while a $^{3}He/^{4}He$ signature of about 8.0 Ra was measured at Turrialba volcano in Costa Rica, which is similar to that of Baru, and reflects possible influence of slab melting, triggered by a change in subduction conditions and the contemporary subduction of the Galapagos hot-spot track below southern Costa Rica and western Panama.

Keywords: Telica volcano; Baru volcano; $^{3}He/^{4}He$; fluid inclusions; CAVA; slab fluids

Citation: Rizzo, A.L.; Robidoux, P.; Aiuppa, A.; Di Piazza, A. $^{3}He/^{4}He$ Signature of Magmatic Fluids from Telica (Nicaragua) and Baru (Panama) Volcanoes, Central American Volcanic Arc. *Appl. Sci.* **2022**, *12*, 4241. https://doi.org/10.3390/app12094241

Academic Editor: Nikolaos Koukouzas

Received: 12 March 2022
Accepted: 20 April 2022
Published: 22 April 2022

1. Introduction

1.1. Geodynamic and Volcanological Framework

The Central American Volcanic Arc (CAVA) results from the subduction of Cocos and Nazca plates beneath the Caribbean (Figure 1), and extends nearly continuously from Guatemala to Panama for more than 1500 km [1]. In contrast to the MORB-like oceanic crust (produced at the East Pacific Rise) that subducts underneath Guatemala to north-western Costa Rica, the oceanic crust formed at the Cocos-Nazca spreading centre, overprinted by Galapagos Hotspot tracks dated 13–14.5 Ma offshore of Costa Rica, is thought to subduct beneath central Costa Rica and Panama [2–4].

The age of the subducting Cocos lithosphere is about 26 Ma along most parts of the subduction zone, except along central Costa Rica, where it is 25 to 17 Ma. The Cocos Ridge, located off the coast of southern Costa Rica (Figure 1), divides the subducting lithosphere into two segments (Cocos and Nazca plates, N-S striking Panama Fracture Zone): the northern is old and cool, while the southern is young and warm [5]. The Cocos materials in the north-western part subduct at a rate of ~80–90 mm/yr [6] and at a moderately steep angle (62.2°) beneath Nicaragua, at 56.9° beneath El Salvador and Guatemala, and at 58.9° beneath Costa Rica [7–9]. In southern and Central Costa Rica, the volcanic arc becomes largely inactive at the Cordillera de Talamanca for ~150 km [10]. Seismic data indicate that a slab window is present beneath southern Costa Rica and Panama, where adakites are erupted [4,7]. This window would be compatible with the numerous hotspot tracks and fracture zones on the subducting Cocos and Nazca plates that clogged the subduction zone, triggered detachment of a major portion of the slab and made it relatively easy to tear.

In Panama, the arc segment does not register volcanic activity, except for three volcanic centres that showed signs of eruptions in recent times: Baru, La Yeguada, and El Valle [11–15]. This arc segment results from the oblique angle subduction of the Nazca plate, which subducts beneath the Panama block at a rate of ~40 mm/yr [6].

According to [16–19], crustal thickness decreases from Guatemala (50–40 km) to Nicaragua (30 km), increases across Costa Rica (up to 45 km), and finally thins again in western and central Panama (~30 km).

1.2. Geochemistry of CAVA and Aims of This Study

CAVA shows significant along-arc geochemical variations in rock composition and age, and in volcanic activity [3,4,20–23], which mostly result from the variations in subduction parameters, such as dip-angle, crustal thickness, extent of sediment underplating, faulting style and subduction erosion [16,20,24]. These parameters control the degree of source melting and determine a variable sedimentary fluid influx from the subducting Cocos plate. Some of the most evident variations in rock geochemistry are represented by trace element proxies for slab fluids (such as Ba/La, U/Th, Ba/Th, and Sr/Ce ratios) being highest in Nicaragua, and lowest in Costa Rica [20,23,25]. The same geochemical tracers indicate that melts beneath Guatemala are generated by the mixing of a Costa Rica MORB-like melt component with Nicaragua-like slab fluid-rich melts [25], while the Quaternary volcanic arc in Panama shows an adakitic composition of still debated origin [26]. It must be mentioned that the Central Costa Rica (i.e., Platanar, Poás, Barva, and Irazu volcanoes) and Panama (i.e., Baru) magmas show an OIB signature that contrasts with that usually observed in the rest of CAVA, which has been attributed to the subduction of the Galapagos seamounts originating along the Galapagos hot-spot track [3,4,21,22].

In terms of volatile geochemistry, most of the studies along CAVA have focused on the composition and fluxes of magmatic gases emitted from the most active volcanoes, such as Turrialba and Poàs in Costa Rica [27–39], Cerro Negro, Masaya, Momotombo and San Cristóbal in Nicaragua [35,40–44], Pacaya in Guatemala [27,45,46]. Several studies have also focused on the composition of noble gases, especially on the $^{3}He/^{4}He$ ratio that is considered a powerful tracer of mantle vs. subducting slab contributions (e.g., [44,47,48]), and of crustal and/or hydrothermal interactions (e.g., [49–53]). Present knowledge on the $^{3}He/^{4}He$ signature along CAVA has been mostly achieved through measurements in fuma-

role and spring gases [27–30,34,42,45,54–61], while much less information is available on fluid inclusions (FI) in olivine (Ol) and pyroxene (Px) crystals [38,44,46,54,62,63]. Irrespective of the huge information available for CAVA, which is probably one of the best studied arcs on Earth, the $^{3}He/^{4}He$ signature of the magmatic source remains unconstrained for many volcanic systems, and its along-arc variations are not well understood. One special concern is that the available $^{3}He/^{4}He$ CAVA dataset is dominated by peripheral gas manifestations and cold springs, in which inferring the mantle source signature is complicated by shallow processes and fluid sources.

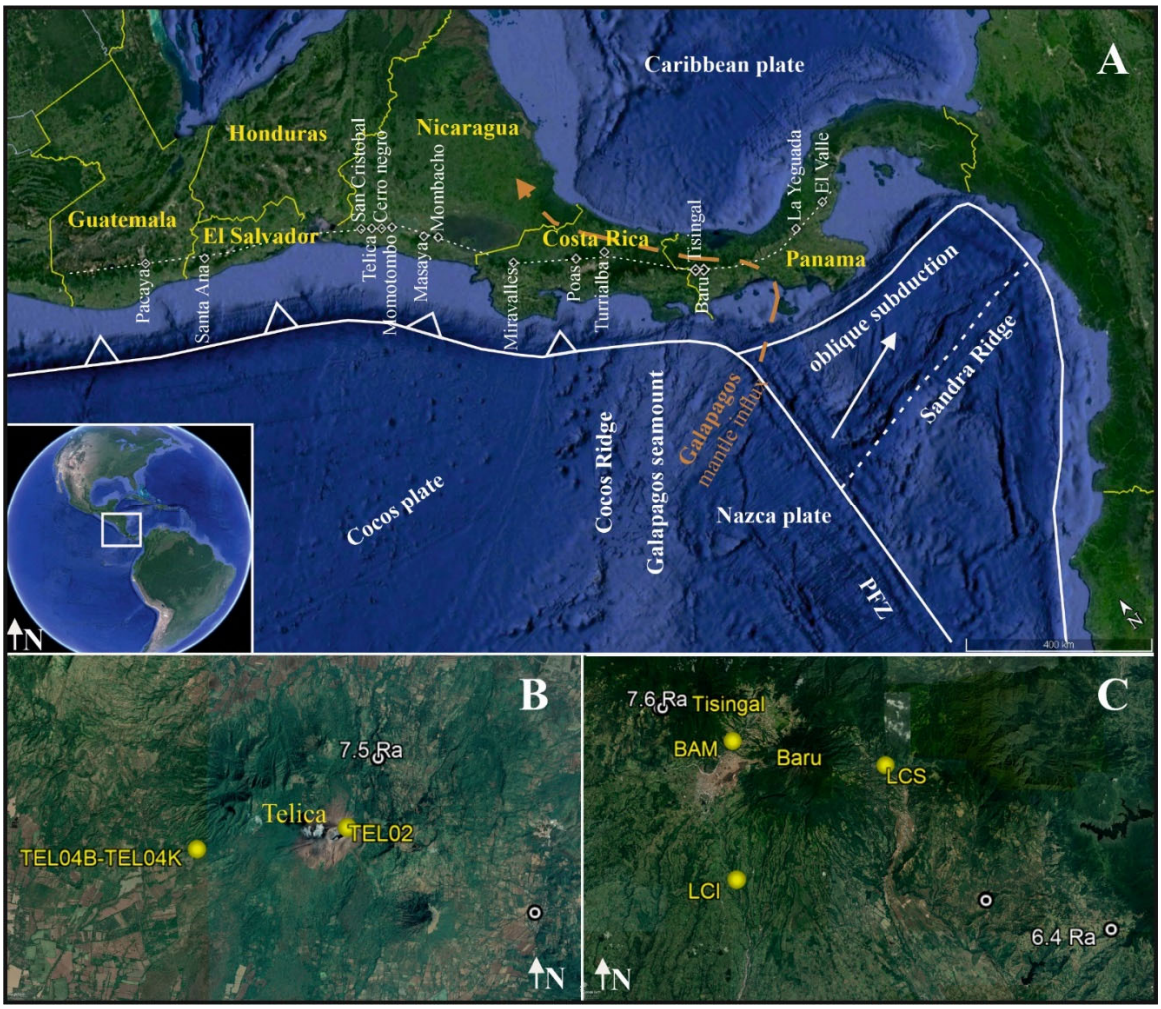

Figure 1. (**A**) Map of the geodynamics of the Central American Volcanic Arc (CAVA), indicating arc-segments from Guatemala to Panama. The white line with the transparent arrows indicates the subduction front direction, while its prolongation to the East indicates the oblique subduction beneath Panama and to the south-east, the Panama fracture Zone (PFZ). The orange dotted line indicates the Galapagos mantle influx inferred by [61]. The white dotted line reports the main location of the volcanic arc front from Guatemala to Panama. The volcanoes mentioned in the text are also reported. (**B**) Inset of map A on Telica volcano (Nicaragua), where our sample location (in yellow) is reported together with the spring gases (in white) studied by [42] with the maximum air-corrected $^{3}He/^{4}He$ (Rc/Ra). (**C**) Inset of map A on Baru volcano (Panama), where our sample location (in yellow) is reported together with the neighboring spring gases (in white) studied by [61] with the maximum air-corrected $^{3}He/^{4}He$ (Rc/Ra). The sampling sites abbreviation is explicated in Table 1.

Table 1. Concentrations (in mol/g) and isotope compositions of noble gases in fluid inclusions of olivine and clinopyroxene from Telica and Baru volcanoes.

Sample ID	Period of Volcanism	Mineral	^{3}He	^{4}He	^{20}Ne	^{40}Ar	^{36}Ar	^{40}Ar*	^{4}He/^{40}Ar*	^{4}He/^{20}Ne	R/Ra	Rc/Ra	Err.	^{40}Ar/^{36}Ar	Err.
			x $1{\cdot}10^{-19}$	x $1{\cdot}10^{-14}$	x $1{\cdot}10^{-15}$	x $1{\cdot}10^{-13}$	x $1{\cdot}10^{-15}$	x $1{\cdot}10^{-14}$					+/−		%
TEL04K	Scoria Telica Superior	Ol	10.8	11.04	4.03	4.5	1.45	2.11	5.23	27.4	7.19	7.27	0.432	310.02	0.97
TEL04K (2)	Scoria Telica Superior	Ol	15.76	16.51	18.56	24.71	8.31	1.52	-	8.9	7.02	7.25	0.249	297.33	0.07
TEL04K	Scoria Telica Superior	Cpx	16.58	17	6.56	5.73	1.9	1.08	-	25.9	7.17	7.25	0.264	301.17	0.27
TEL04K (2)	Scoria Telica Superior	Cpx	12.09	12.36	7.97	17.23	5.73	3.02	-	15.5	7.19	7.33	0.483	300.77	0.46
TEL04B	Scoria Telica Superior	Ol	4.59	4.69	4.5	3.93	1.28	1.4	3.36	10.4	7.2	7.41	0.289	306.38	0.16
TEL04B (2)	Scoria Telica Superior	Ol	6.16	6.37	9.68	6.09	2	1.9	3.36	6.6	7.11	7.43	0.239	305.01	0.09
TEL02	Post-1970s	Cpx	6.77	7.43	18.27	14.05	4.43	9.75	0.76	4.1	6.7	7.21	0.273	317.53	0.08
TEL02 (2)	Post-1970s	Cpx	6.86	9.13	28.98	19.19	6.39	2.93	-	3.2	5.52	6.06	0.392	300.09	0.25
LCI	La Cuesta Inferior	Ol	4.41	4.21	4.42	23.7	7.3	21.4	0.2	9.5	7.7	7.94	0.346	324.84	0.09
LCI (2)	La Cuesta Inferior	Ol	3.09	3.18	0.17	8.74	2.51	13.19	0.24	184	7.14	7.15	0.463	348.07	0.64
LCI	La Cuesta Inferior	cpx	0.53	0.87	6.82	8.54	2.61	8.15	0.11	1.3	4.45	5.68	0.687	326.68	0.11
BAM	Bambito	cpx	0.17	0.37	2.66	11.65	3.44	14.74	0.03	1.4	3.39	4.19	0.676	338.32	0.09
LCS	La Cuesta Superior	cpx	0.3	0.53	5.16	5.04	1.1	18.05	0.03	1	4.19	5.77	0.611	460.24	0.42

In order to help in filling this gap of knowledge, we present in this work the first $^3He/^4He$ results for FI in Ol and Px separated from rocks of two poorly studied volcanic systems of CAVA: Telica, in Nicaragua, and Baru, in Panama. The study of FI in Ol and Px, together with their mineralogical and petrological features, provides the opportunity to look directly at the magmatic fluids degassed in the plumbing system, thus providing complementary information with respect to fumarole and hydrothermal gases.

Telica is among the most active open-vent degassing volcanoes of basaltic andesite composition in the Central American Volcanic Arc (CAVA) [31,64]. Its seismic activity and major gas emissions have been closely examined over recent years [65]. Volcanic activity includes violent strombolian explosions and minor vulcanian events, interspersed with frequent minor phreatomagmatic events [65].

Baru is the most recent stratovolcano in Panama with documented historic activity (1550 ± 10 years; [66–68]). The summit of the volcano rises at 3374 m above sea level, the whole morphology constitutes a massive composite stratovolcano of between 400–450 km^3 [15,66–68]. Volcanic rock activity in the Baru region has been recorded since the early Tertiary [67,68] period, and the main volcano building stages in the Pleistocene-to-Holocene [12] include large explosive eruptions.

These two volcanoes, apart from being poorly studied in terms of $^3He/^4He$ of magmatic gases, are located in contrasting segments of the CAVA, as Telica magmatism is strongly influenced by subducting sediment fluids, while Baru is located in the Quaternary arc segment of Panama, considered still active but originating from the oblique subduction of the Nazca plate that includes the Galapagos seamount.

We constrained the $^3He/^4He$ signature of these magmatic systems and put our results in the context of previous results obtained from other CAVA volcanic systems. This information is finally integrated with previous knowledge on rock geochemistry along CAVA. This allows us to evaluate the possible modifications of the pristine $^3He/^4He$ of the mantle portions beneath the studied volcanoes (e.g., [69–71]), in response to subduction parameters and crustal thickness.

2. Samples and Methods

For this study, we selected 3 rock samples from the Telica volcano in Nicaragua (TEL02, TEL04B and TEL04K) and 3 samples from the Baru volcano in Panama (BAM, LCI, LCS) (Figure 1). The most mafic samples were selected, considering that Ol and Px are the most suitable for the study of noble gases (He, Ne, Ar) in FI.

Rocks from Telica were taken from a suite of samples already studied by [72] for their petrography and mineral-rock composition. These samples belong to the 1982 eruption (TEL02) and to scoria fragments taken from the Scoria Telica Superior (STS) deposit on the west and south-west flanks of Telica (TEL04B, TEL04K). The 3 February 1982, eruption (VEI = 2) produced bombs that can be found at 500–1000 m distance from the NE crater rim [73,74], and contain a mineral assemblage of Px > Ol, with dominant plagioclase and accessory magnetite [72]. The STS has a minimum age at 2150 ± 150 yrs B.P. [74]. The STS samples are classified by [72], based on their stratigraphic positions. Samples TEL04B, TEL04K are dark to grey in colour, and are made up of small to medium size lapilli with minor fine ash. The fragments are highly vesicular with mineral assemblage similar to the February 1982 eruption [75]. TEL04B has large yellow Ol (>4–12 mm). It also contains larger Px [72].

Rocks from the Baru volcano were collected during field work in 2016. The analysed samples refer to some episode of the Pleistocene-to-Holocene effusive activity, and were chosen according to stratigraphic description and the petro-geochemistry of the lavas [12,13]. The sample from La Cuesta Inferior (LCI) represents a basaltic andesite lava flow at the base of the La Cuesta unit, with an age of 0.213 Ma [13]. The flow is compact with grey colour groundmass, and porphyric fabric with some aggregates that contain less than 5–10% Ol of 1–4 mm diameter. Prismatic Px is found in similar proportions (5–8%). The sample from La Cuesta Superior (LCS) represents a basaltic andesite lava flow with columnar joints, for

which previous studies establish an age of 0.122 Ma [13]. The sampling site is located on the eastern flank of the volcano, close to the Bajo Mono North exit (Lat. N 8°48′15.30″/Long. W 82°27′10.10″) and at an altitude of 1287 m. The LCS is the Upper layer of La Cuesta Unit, a voluminous, 13 m thick lava flow unit that outcrops along the "Río Caldera" river in the Bajo Mono area. It exhibits columnar joints of 55 cm diameter, a compact aspect, a grey colour groundmass, and porphyric fabric with some aggregates that generally contain more Ol than LCI (10–12%). The Px crystals (5%) have euhedral prismatic shapes with a long axis of 5 mm. The Bambito unit (BAM) represents an andesite lava unit found NW of Baru, and has an approximate age of 0.122 to 0.011 Ma [13]. The sampling site is found between the Nuevo Bambito and Volcan villages, west of Cerro Aguacate, on road 418 along the Río Chiriquí Viejo (Lat. N 8°49′46.98″/Long. W 82°36′53.36″). The rock was sampled at 1743 m altitude, and was taken from a slightly weathered massive outcrop. It contains very few ferromagnesian minerals, such as a 4–6% euhedral prismatic Px with a green-turquoise colour (no Ol was observed on thin sections).

Major and trace element bulk-rock analyses of the Baru samples were performed at the Activation Laboratories (Ancaster, Canada) following preparation techniques and analytical procedures already described by [38,46,72,76,77]. Data are reported in Table S1.

Rock fragments containing phenocrysts were prepared on Crystal Bond™ resin, then polished over one side for glass rim or distinct glass fragments. Ol and Px, separated by hand picking, were all prepared on different mounts after using abrasives and polishing down to 6-, 3-, and 1-µm diamond powder fractions.

Mineral chemistry was determined in the HPHT (high-pressure/high temperature) laboratory of the Istituto Nazionale di Geofisica e Vulcanologia (INGV) in Rome, by using a JXA-8200 electron microprobe (EMPA). The analytical conditions and uncertainty are the same as already reported in recent studies (i.e., [44,72,76,77]). Mineral chemistry was measured on the surface of thin sections for the Baru samples. In total, 77 spots were performed on cores and rims from phenocrysts, representing 68 Px and 9 Ol. The results are reported in Table S2.

The rock samples to be analysed for their FI were crushed and sieved several times until a homogeneous grain size of 0.5–1.0 mm was obtained, except for the TEL04B sample, from which we hand-picked Ol and Px crystals in the fraction of 1.0–2.0 mm. Ol and Px were separated from scoriae and less-dense minerals (e.g., plagioclase, amphiboles) by using sodium polytungstate liquid. Minerals were washed with deionized water and acetone. The selected crystals were finally weighted (0.1–1.5 g) and loaded into a stainless-steel crusher. Further details on the protocol of rock and mineral preparation can be found in Rizzo et al. [49,78,79].

Noble gases trapped inside FI were released by in-vacuo single-step crushing. This procedure is the most conservative, because it minimises the contribution of cosmogenic ^{3}He and radiogenic ^{4}He possibly grown/trapped in the crystal lattice (e.g., [63,69–71]). Gas released from the mechanical fragmentation of crystals was cleaned in an ultra-high vacuum purification line, allowing all gas species, except noble gases, to be removed. Helium isotopes (^{3}He and ^{4}He) and ^{20}Ne were measured separately by two different split-flight-tube mass spectrometers (Helix SFT-Thermo). The analytical uncertainty of the He isotopic ratio is generally <11%. Argon isotopes (^{36}Ar, ^{38}Ar and ^{40}Ar) were analysed by a multi-collector mass spectrometer (GVI Argus), with an analytical uncertainty generally <1.5%. The ^{3}He/^{4}He ratios are expressed as R/Ra (where Ra is the ^{3}He/^{4}He ratio of air, which is equal to $1.39 \cdot 10^{-6}$). The R/Ra values were corrected for atmospheric contamination based on the ^{4}He/^{20}Ne ratio (e.g., [80]) and expressed hereafter as Rc/Ra values. The uncertainty in the determinations of He, Ne, and Ar elemental concentrations was less than 5%. Typical blanks for He, Ne and Ar were $<10^{-15}$, $<10^{-16}$ and $<10^{-14}$ mol, respectively. Further details on sample purification and analytical procedures are available in Rizzo et al. (2021 and references therein).

^{40}Ar was corrected for air contamination ($^{40}Ar^*$) in samples showing $^{40}Ar/^{36}Ar > 305$, assuming that the measured ^{36}Ar was entirely of atmospheric origin as follows:

$$^{40}Ar^* = {}^{40}Ar_{sample} - [{}^{36}Ar_{sample} \times ({}^{40}Ar/{}^{36}Ar)_{air}]. \quad (1)$$

3. Results

3.1. Bulk Rock and Mineral Chemistry

The sampling location and major and trace-elemental compositions of the samples are presented in Table S1. For the Telica volcano, the major oxide description of the samples selected for this volcano was taken from [72]. Whole-rock compositions at Telica range from basaltic to andesitic (SiO_2 = 50.9–58.6 wt%; K_2O = 0.84–1.43 wt%) and plot in the field of calc-alkaline (CA) to high-potassium calc-alkaline (HKCA) rocks [72]. These fall within the compositional ranges reported in the literature (50.8–53.5 wt% SiO_2; 0.9–1.1 wt% K_2O; e.g., [20,81,82]). The basalts and basaltic andesites are enriched in large ion lithophile elements (LILE: Cs, Rb, Ba, La, etc.) relative to N-MORBs (Table S1). Most samples have moderate to strong high field strength element depletion (HFSE: Ta, Nb, Zr, Hf), and display generally lower Hf, Zr and Ti contents than N-MORB and E-MORB averages [83]. The normalised pattern also exhibits Ti and Zr anomalies relative to N-MORB [68].

The Baru volcanic rock samples are basaltic andesites of the CA series (Table S1) [12]. Samples from La Cuesta are characterised by high Mg# [13]; within the high magnesium andesite field of 55–70 Mg#. The basaltic andesites are less enriched in large ion lithophile elements LILE relative to N-MORBs. Most samples have moderate to strong high field strength elements depletion (HFSE: Ta, Nb, Zr, Hf), with Nb = 5–11 ppm and Ta = 0.5–0.8 ppm, in line with adakitic characteristics (Supplementary Material S5).

Mg# and Forsterite (Fo) contents for both Telica and Baru are illustrated in Figure S1. At Telica volcano, green clinopyroxenes on thin sections are identified as augite (Wo_{36}-$En_{44}Fs_{19}$) with Mg# values (Mg/(Mg + Fe) of 71%. In sample TEL02, Px has dark green translucid tones, distinct cleavage, and is <4 mm. On thin sections, these were identified as augite ($Wo_{41–42}En_{38}Fs_{20}$) with Mg# values (Mg/(Mg + Fe) = 71–72% and also contain iron oxides and Ol. The Ol is of a green transparent to pale green tone (some yellow in TEL02), generally <2 mm in size and with small plagioclase intergrowths. At Baru, only one out of 11 crystals of augites from sample LCI recorded strong normal zoning from core-to-rim (81 to 78% Mg#). These augites are observed in intergrowth with plagioclase phenocrysts of the same size, occasionally grouped with glomeroporphyric textures. The Ol have $Fo_{74–90}$ compositions, and two are normally zoned (Fo_{85} to Fo_{81} and Fo_{76} to Fo_{74}). The Mg# value of Px decreases from LCS and LCI to Bambito (Mg# 60–70). Px are slightly more variable in LCS ($Wo_{42–48}En_{41–49}Fs_{6–13}$) with Mg# of 74–89%. Normal zonation was recorded in 3/13 while reverse zoning was recorded in 2/13 crystals. In sample BAM, some green clinopyroxenes on thin sections were identified as augites ($Wo_{40–45}En_{41–48}Fs_{8–13}$) with Mg# values (Mg/(Mg + Fe) = 77–85%. Most of the augite crystals are present as phenocrysts of large diameter (>2–4 mm) and contain concentric oxides and glass inclusions.

3.2. Isotope Composition of Noble Gases in Fluid Inclusions

12. aliquots of Ol and Px crystals were separated from the 6 Telica and Baru samples, and selected for He, Ne and Ar isotope measurements in FI (Table 1).

For the Telica volcano, the ^4He concentrations [He] measured in samples TEL02, TEL04K and TEL04B varied significantly (Figure 2). In Ol they ranged from $4.69 \cdot 10^{-14}$ mol/g to $1.10 \cdot 10^{-13}$ mol/g. In Px, [He] they ranged from $7.43 \cdot 10^{-14}$ mol/g to $1.70 \cdot 10^{-13}$ mol/g. The lowest ^4He contents were observed in sample TEL04B (Ol), while the Px of TEL04K was typically the most [He] rich (Table 1). Ne and Ar in Ol had ranges of $4.03 \cdot 10^{-15}$ mol/g–$1.86 \cdot 10^{-14}$ mol/g and $3.93 \cdot 10^{-13}$ mol/g–$2.47 \cdot 10^{-12}$ mol/g, respectively. Ne and Ar were found at levels of $6.56 \cdot 10^{-15}$–$2.90 \cdot 10^{-14}$ mol/g and $5.73 \cdot 10^{-13}$–$1.92 \cdot 10^{-12}$ mol/g respectively in Px (Table 1). The $^{40}Ar/^{36}Ar$ values were from 297.0 to 318.0 in all samples, slightly higher than typical atmospheric signatures ($^{40}Ar/^{36}Ar$ = 295.5; [84]). $^4He/^{20}Ne$ ratios varied

in the 3.2–27.4 range (Figure 3), with the highest values measured in samples TEL04K, TEL04B (the atmospheric $^{4}He/^{20}Ne$ is 0.318; [84]. In samples from Telica, $^{40}Ar^{*}$ was in the range 1.08–9.75·10^{-14} mol/g (Table 1).

For the Baru volcano, [He] concentrations measured in FI from Ol and Px of LCI, LCS and Bambito samples were generally 10 times less than in Telica crystals (Figure 2). In Ol, [He] ranged from 3.18·10^{-14} mol/g to 4.21·10^{-14} mol/g, while Px varied from 3.70·10^{-15} mol/g to 8.71·10^{-15} mol/g (Figure 2). The lowest He content was observed in Px from LCI, while Ol were typically the most [He] rich. Ne and Ar in Ol had ranges of 1.73·10^{-16} mol/g–4.42·10^{-15} mol/g and 8.74·10^{-13} mol/g–2.37·10^{-12} mol/g, respectively (Table 1). Neon and Argon were found at levels of 2.66·10^{-15}–6.82·10^{-15} mol/g and 5.04·10^{-13}–1.16·10^{-12} mol/g, respectively in Px. $^{40}Ar/^{36}Ar$ values were from 324.8 to 460.2. The $^{4}He/^{20}Ne$ varied in the range 1.0–184.0 with the highest value measured in Ol from LCI (Figure 3). In samples from Baru, $^{40}Ar^{*}$ varied between 8.15·10^{-14} and 2.14·10^{-13} (Table 1).

The $^{3}He/^{4}He$ corrected for atmospheric contamination (Rc/Ra) in Ol samples from Telica varied from 7.25 Ra to 7.43 Ra, while in Px from 6.06 Ra to 7.33 Ra (Figures 2 and 3; Table 1). In the Baru volcano, Ol samples varied from 7.14 Ra to 7.94 Ra, while Px from 4.19 Ra to 5.77 Ra.

Due to the strong atmospheric contamination shown by the $^{4}He/^{20}Ne$ and $^{40}Ar/^{36}Ar$ values, the bias between Rc/Ra and R/Ra values was between 0.08 and 0.79 Ra, except for cpx of samples LCI and LCS where it reached 1.24 and 1.58 Ra, respectively (Table 1).

At Telica, $^{4}He/^{40}Ar^{*}$ ratios varied between 0.76 (in cpx from TEL 02) and 5.23 (in Ol from TEL04K), while at Baru they were between 0.03 (in cpx from BAM and LCS) and 0.24 (in Ol from LCI). The $^{4}He/^{40}Ar^{*}$ from Telica were within the typical mantle production ratio (1–5, [85] and the range of magmatic gases (e.g., [38,49,51,52]. In contrast, those from Baru reflected an early stage of degassing ($^{4}He/^{40}Ar^{*}$ = 0.2) and a partial loss of helium ($^{4}He/^{40}Ar^{*}$ = 0.03–0.11) as testified by the contemporary low Rc/Ra values (Table 1).

Except for the replicate measurement of cpx from TEL02, where the presence of some scoria around the crystals probably led to the addition of radiogenic ^{4}He that lowered the $^{3}He/^{4}He$ to 6.06 Ra, Ol and Px from Telica showed isotopic equilibrium in the samples (Figure 2). This was not the case for the Baru samples, where cpx showed systematically lower Rc/Ra values than Ol. This was also the case for $^{4}He/^{40}Ar^{*}$ ratios, that showed the lowest values (0.03 and 0.11) in samples showing the lowest Rc/Ra. Considering that cpx from Baru also showed the lowest He content, the low Rc/Ra and $^{4}He/^{40}Ar^{*}$ values were reasonably due to a diffusive loss of helium from the crystals (Figure 2). This is not unusual as it has been observed in several volcanic systems worldwide, irrespective of geodynamic setting or magma chemistry [63,70,71,86]. For this reason, the replicate measurement of cpx from TEL02 and the cpx from LCI. LCS and BAM were excluded from the following discussion.

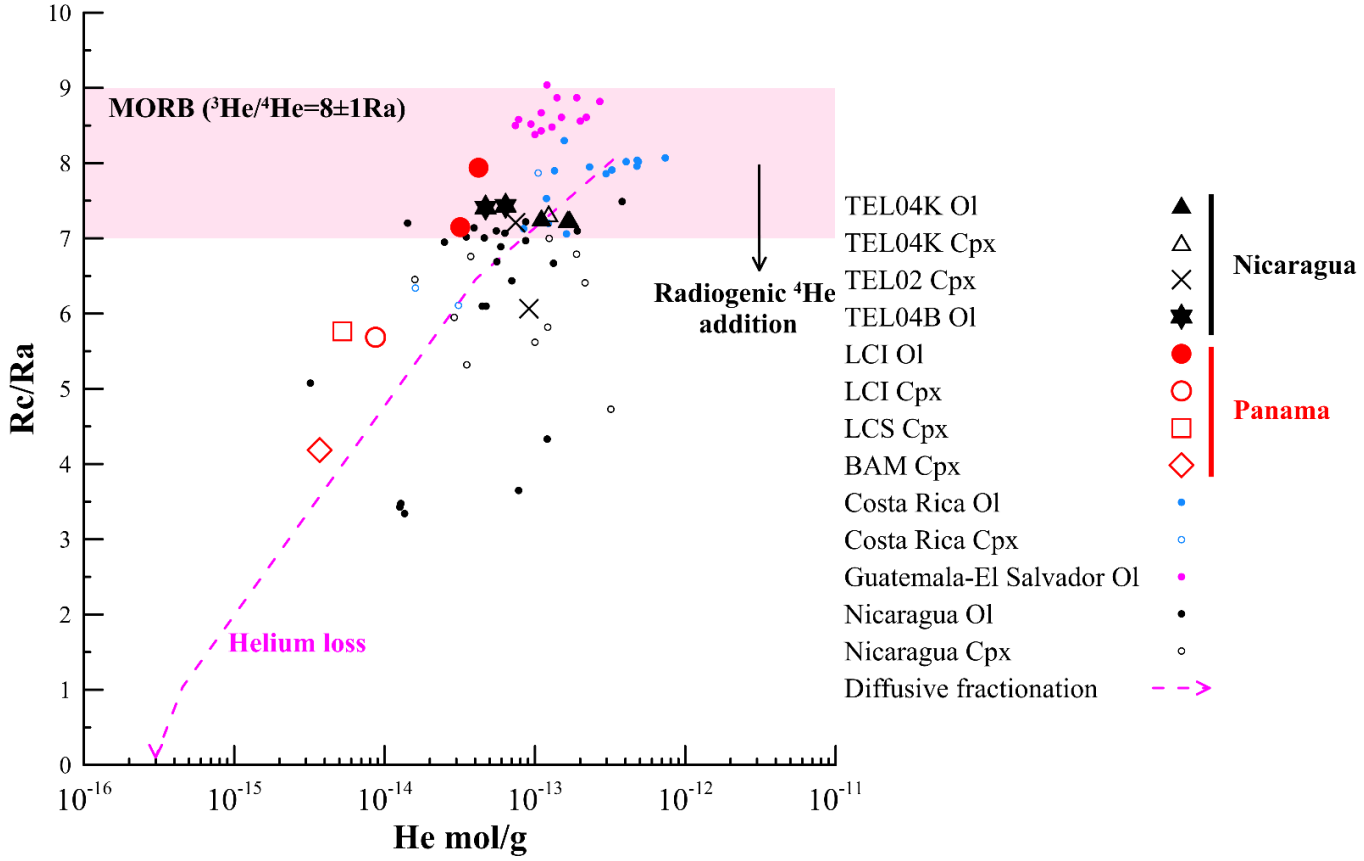

Figure 2. He concentration in fluid inclusions (FI) in mol/g versus air-corrected $^{3}He/^{4}He$ (Rc/Ra) ratio. Data of FI hosted in olivine (Ol) and clinopyroxenes (Cpx) are distinguished for the Telica (black symbols) and Baru (red symbols) samples. Additional data of FI along CAVA are reported for comparison [38,46,54,62,63,72] and distinguished (with different colors) per mineral phase and arc-segment. Due to the presence of a few data and their vicinity, Guatemala and El Salvador are considered and discussed in the text as a unique segment. More details on the source data are reported in the Supplementary Table S4. Mid Ocean Ridge Basalt (MORB) range of $^{3}He/^{4}He$ is from [87]. The pink dashed line represents the path of diffusive fractionation due to helium loss from the crystals, taking into account the diffusion coefficient (D) of ^{3}He and ^{4}He (D_{3He}/D_{4He} = 1.15 in solid mantle; see [79] for more details). Starting magmatic composition is: $^{4}He = 3 \times 10^{-13}$ mol/g and $^{3}He/^{4}He$ = 8.0 Ra. These values were chosen considering mean compositions of Costa Rican Ol FI, only to show the behaviour of the expected path.

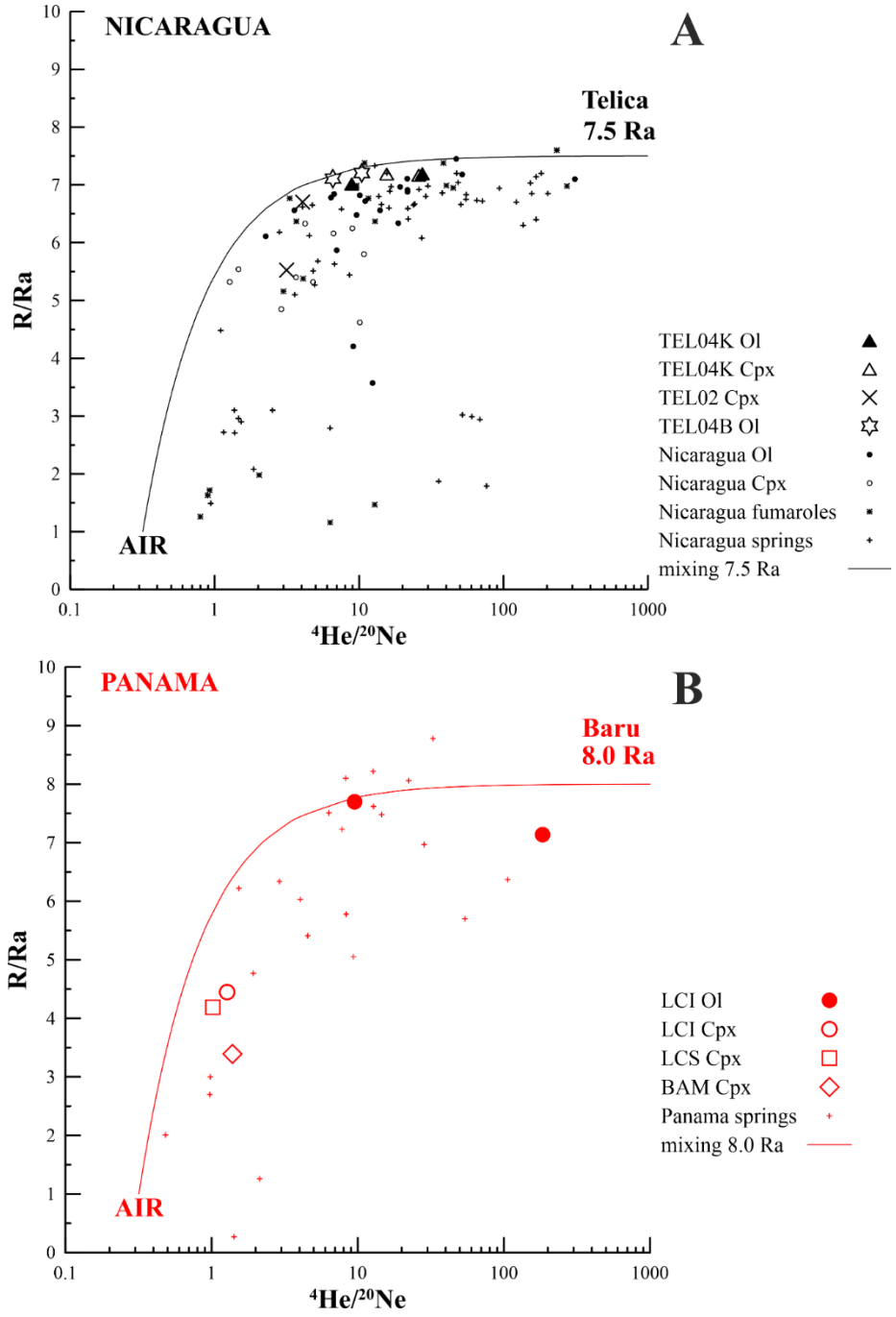

Figure 3. ^{4}He/^{20}Ne versus ^{3}He/^{4}He (R/Ra) in FI, fumaroles and springs from Nicaraguan (**A**) and Panamanian (**B**) segments of CAVA. Fumarole and springs data from previous studies are reported for comparison [27–30,34,38,42,45,48,54–61]. More details on the source data are reported in Supplementary Table S3. The black and red lines indicate binary mixing between air and two hypothetical magmatic/mantle sources assumed below the respective segments of CAVA.

4. Discussion

Light noble gases are powerful geochemical tracers of volatiles' composition and origin, due to their inert physical-chemical features and the different origins of their isotopes. Ne and Ar isotopic ratios more commonly provide information on the extent and origin of the atmosphere-derived contamination that often occurs in natural fluids. In subduction-

related settings, revealed Ne and Ar isotopes have been useful in recognising the recycling of atmospheric components into the mantle wedge, likely in the form of air-saturated oceanic water trapped in clay minerals and sediments [52,53,78,79,88–94]. This is due to the higher concentration of Ne and Ar in atmosphere (Ne~18 ppm, Ar~9300 ppm) [84] than in magmatic, mantle and crustal fluids, where Ne is normally present in a few ppb and Ar in ppm. Instead, helium is used to distinguish the origin of fluids and to recognise contamination or mixing processes occurring at mantle or crustal depths (e.g., [49–51,78,79,95–100]). This is due to the distinct origins of its two isotopes, whereby ^{3}He is cosmogenic, not renewed and stored in the Earth's interior, while ^{4}He originates from the radioactive decay of U and Th in the crust [84].

In subduction-related settings, the ^{3}He/^{4}He ratio of the mantle wedge, and thus of magmatic/volcanic gases, is normally expected within the MORB range (8 ± 1 Ra) [87], due to the fact that the oceanic crust originally has a MORB-like signature and early models of noble gases hypothesised a subduction barrier for their recycling into the mantle [101]. However, this is not always observed in arc volcanoes on Earth, where ^{3}He/^{4}He values lower than 7.0 Ra are often found [70,102–104]. Nevertheless, it must be noted that it is only at volcanic arcs, where continental crust is involved in the subduction, that slab fluids are likely to significantly play a game in determining ^{3}He/^{4}He values of <<7.0 Ra (e.g., Italy, [47,105]). Elsewhere, arc volcanoes showing a ^{3}He/^{4}He signature lower than MORB are likely to primarily reflect contamination of magma/magmatic gases in the crust by radiogenic ^{4}He addition. This is especially the case for datasets based on measurements carried out in spring gases sampled far from the main eruptive centres, and/or in inactive volcanoes (e.g., [52,53] and references therein [102]). This is the reason why, in recent years, most of studies aimed at constraining the ^{3}He/^{4}He signature of the wedge below arc volcanoes have focused on the study of FI in olivine and pyroxene crystals. It is important to remember that minerals growing and crystallizing during igneous processes are expected to trap fluid and melt inclusions. FI can be either primary or, more frequently, secondary in developing along crystal fractures or growing directions. Other fluids are also trapped and appear as contraction bubbles of melt inclusions (i.e., shrinkage bubbles). These fluids may preserve a more primitive volatile signature than volcanic and hydrothermal gases.

Recent studies have put the accent on the possible influence of slab fluids in lowering ^{3}He/^{4}He values in the wedge [38,44,53], although the final isotopic signature may remain well within the MORB range.

Here we provide the first ^{3}He/^{4}He measurements in FI of minerals from Telica and Baru volcanoes, for which only a few measurements in spring gases were available until now. We constrain the helium magmatic signature of these two volcanoes, and put the results in context to evaluate the possible role played by slab and crustal fluids.

4.1. ^{3}He/^{4}He Signature of Telica and Baru Magmatic Fluids

At Telica volcano, the highest ^{3}He/^{4}He values in FI were measured in samples TEL04B and TEL04K, which yielded Rc/Ra values up to 7.43 Ra (Figures 2 and 3). Following the detailed petrological study carried out by [72], the crystallization depth of Ol and Px from TEL04K and TEL04B is compatible with magma storage zone at 5–15 km depth, where moderate to low extents of magma differentiation and mixing explain the melts and mineral variability. TEL04K shows a large difference between the average Fo contents of Ol (Fo% = 80.5 ± 3.9) and the Mg# of Px (71.2 ± 3.3) (Figure S1), which implies different crystallisation stages [72]. Instead, sample TEL02, in which Ol is absent, is compatible with increasing extents of magma differentiaton and degassing at shallow depth (<2.4 km). It is worth noting that Ol and Px from the Telica samples show a comparable range of values (7.25–7.43 Ra and 7.21–7.33 Ra, respectively) (Figure 2), which indicates that mixing and differentiation processes occurring within the crustal plumbing system of the volcano do not modify the ^{3}He/^{4}He signature of fluids trapped in the minerals to any major extent.

Previous studies reporting ^{3}He/^{4}He measurements for the Telica volcano [42] are limited to spring gases and waters. Shaw et al. (2003) studied a few samples taken in a

water spring and in bubbling hot gases collected on the flank of the volcano and in the San Jacinto fault system that is associated with Telica. These samples yielded $^{3}He/^{4}He$ values in the range 2.9–7.5 Ra (Figure 3 and Table S3). The highest Rc/Ra value is comparable to our novel FI results, confirming 7.5 Ra as being the representative He signature of the magmatic source below Telica (Figure 3).

At Baru volcano, the highest $^{3}He/^{4}He$ values in FI were measured in Ol from sample LCI, which yielded Rc/Ra values up to 7.94 Ra (Figure 2). These crystals show Fo content of 79.1 ± 1.05 that testifies to a moderate-to-low extent of differentiation, as observed for Telica samples from STS.

Studies reporting measurements of $^{3}He/^{4}He$ on Baru volcano, or close to it, were totally absent until recent work by [61], who first reported some measurements in hydrothermal gases and waters located in the proximity of the volcano. Around Baru, the authors found $^{3}He/^{4}He$ up to 6.4 Ra (Figure 3 and Table S3). This value is lower than what we obtained in FI, suggesting that spring gases are contaminated by crustal fluids containing radiogenic ^{4}He, a fact that is consistent with the current quiescency (and hence reduced magmatic gas transport) of Baru [12]. We thus argue that 8.0 Ra is likely representative of the local magmatic source (Figure 3).

Therefore, the $^{3}He/^{4}He$ signatures of the Telica and Baru volcanoes fall within the MORB range (8 ± 1 Ra; [87], while being above the average ratio (5.4 ± 1.9 Ra) proposed for global arc volcanism [70] (Figure 2).

4.2. Crust Thickness vs. $^{3}He/^{4}He$ Variations along CAVA

We now consider the $^{3}He/^{4}He$ signatures constrained above for Telica and Baru volcanoes in the context of previous results for the Nicaraguan and Panama arc segments, respectively. To do this, we start evaluating the $^{4}He/^{20}Ne$ vs. R/Ra plot that allows us to report all the available data from FI, fumarole and spring gases together (Figure 3).

Among Nicaraguan volcanoes (Figure 3A), data for fumarole gases (n = 29) are available for Mombacho, Masaya, Momotombo, Cerro Negro and San Cristobal volcanoes ([42,57,58,60]), spring gases and waters (n = 46) for Mombacho, Masaya, Momotombo, Telica and Conseguina [42,56–58], FI in ol and/or cpx (n = 36) for Momotombo, Cerro Negro and San Cristobal ([34,44,62,63] (Tables S3 and S4). We filtered this dataset by only considering data from fumarole gases and FI that, being typically less affected by shallow secondary processes, are therefore more representative of the $^{3}He/^{4}He$ signature of the magmatic/mantle source [38,46,48–53,72,76,93,94]). For those volcanoes where only spring gas data are available, we only considered the samples showing Rc/Ra values within the MORB range (i.e., >7 Ra). Then, considering the maximum $^{3}He/^{4}He$ value(s) measured in each volcanic system, we derived the following magmatic signatures for the Nicaraguan volcanoes: Mombacho 7.6 Ra, Masaya 7.2 Ra, Momotombo 7.4 Ra, Cerro Negro 7.4 Ra, Telica 7.5 Ra, San Cristobal 7.2 Ra.

Much less $^{3}He/^{4}He$ information is available for the Panama arc segment (Figure 3B). In detail, Bekaert et al. (2021) sampled spring gases and waters (n = 31) located at a longitude between 79.8 and 82.7 and a latitude between 7.4 and 8.8. Apart from some springs (n = 7) located clearly far from the arc segment, the other samples were taken in proximity of the Tisingal, Baru, La Yeguada and El Valle Quaternary volcanoes, showing $^{3}He/^{4}He$ values as high as 7.6 Ra, 6.4 Ra, 8.9 Ra and 8.4 Ra, respectively [61]. For the Baru volcano, spring gases likely suffer an addition by radiogenic crustal-derived ^{4}He, as our FI measurements yielded a magmatic signature of 8.0 Ra (Figure 2).

When considering the entire Nicaraguan and Panamanian segments, we observed that the former has a $^{3}He/^{4}He$ of 7.2–7.6 Ra, the latter of 7.6–8.9 Ra (Figures 2 and 3). Both ranges are within the typical MORB values (8 ± 1 Ra; [87], but the Panamanian volcanoes fall right at the upper MORB limit. This high $^{3}He/^{4}He$ signature for volcanism in Panama was first brought to light by [61], who proposed that a ratio of 8.9 Ra is likely to under-estimate the real mantle signature because of the potential addition of crustal He to deeply rising magmatic fluids upon their transit through/storage in the crust. In [61],

it was proposed that the crust may contribute up to 14–66% of He discharged by Panama gas/spring manifestations which, if correct, would implicate a pristine (pre-mixing with crustal fluids) mantle He signature of ≥10.2 to ~26 Ra. This ^{3}He-rich signature would be caused by the infiltration of a Galapagos plume-like mantle through a slab window that opened ~8 Ma underneath Panama [61].

Recent work has demonstrated that crustal processing (^{4}He addition) can indeed play a role in lowering the ^{3}He/^{4}He signature of mantle-derived magmatic/volcanic gases of arc volcanoes that developed on continental crust [52,53]. We therefore attempt to evaluate this effect for Nicaragua/Panama by looking at the relationship between crustal thickness and He isotopes (Figure 4).

We note (Figures 4 and S2) that the Panamanian segment volcanoes developed above a ~30 km of continental crust [19,61,106], while in Nicaragua the crust is ~34–35 km thick. Although the crust is, thus, slightly thicker below Nicaragua than underneath Panama, it remains that the two areas have the lowest crustal thicknesses reported for CAVA (Figures 4 and S2, [16]). We therefore extend the crustal thickness vs. magmatic ^{3}He/^{4}He analysis to all CAVA volcanoes (including other segments, such as Guatemala, El Salvador and Costa Rica) for which data are available [27–30,34,38,42,44–46,48,54–61]. In this exercise, we adopted the same data selection criteria discussed above, by considering only the maximum ^{3}He/^{4}He ratios among fumarole gases and FI, and spring gases with Rc/Ra values within MORB range. Based on this data selection, we obtained the following Rc/Ra signatures for the volcanoes: Pacaya (Guatemala) 9.0 Ra, Santa Ana (El Salvador) 7.6 Ra, Miravalles (Costa Rica) 7.4 Ra, Poas (Costa Rica) 7.6 Ra, Telica (Costa Rica) 7.2 Ra, Turrialba (Costa Rica) 8.3 Ra. The results, illustrated in Figure 4, demonstrate that there is no obvious relationship between magmatic ^{3}He/^{4}He and crustal thickness. In particular, we note that Rc/Ra > 7.6 are not restricted to Panama (Baru, La Yeguada, El Valle), but are indeed rather common to Costa Rica (Turrialba) and Guatemala (Pacaya), where crust thickness is far higher (~45 km) than underneath Baru. Based on all this evidence, we conclude that crustal processing of magmas/gases is unlikely to be a primary control factor on the distinct ^{3}He/^{4}He signatures of the Panamanian and Nicaraguan arc segments, as well as between the other arc volcanoes of CAVA. If this was the case, then some relationship with crustal thickness should be observed, as, for example, was recently found in the Andes [53]. We do not exclude, however, that some local and small addition of radiogenic ^{4}He occurs at places along the arc.

4.3. Slab Influence on along-CAVA ^{3}He/^{4}He Variations

CAVA is one of the most studied subduction-related settings on Earth, and this favoured the identification of clear geochemical patterns along the ~1500 km arc [3,4,20–23,107]. Some of the best documented variations include those based on the analysis of volcanic rock geochemistry, and especially the trace element proxies for slab sediment fluids (such as Ba/La, Ba/Th, U/Th ratios; Figures S2 and S3). In detail, Ba/La and U/Th have been found to be the highest in Nicaragua, and lowest in Costa Rica and Panama [4,11–13,20,23,108,109]. It must be mentioned that volcanoes in central-southern Costa Rica (i.e., Platanar, Poás, Barva, and Irazu volcanoes) and Panama (i.e., Tisingal, Baru, La Yeguada and El Valle) show an OIB magma signature that contrasts with that usually observed in the rest of CAVA (Figures S2 and S3). This specific feature has been attributed to the subduction of Galapagos seamounts originating along the hot-spot track [3,4,21,22]. Adakitic magmas found at Turrialba and in Panamanian Quaternary volcanoes are thought to result from the direct melting of the subducting oceanic crust rather than of the wedge [3,4,10,67,108–114], although other hypotheses have also been set out to explain this composition [13–15,61,115–120].

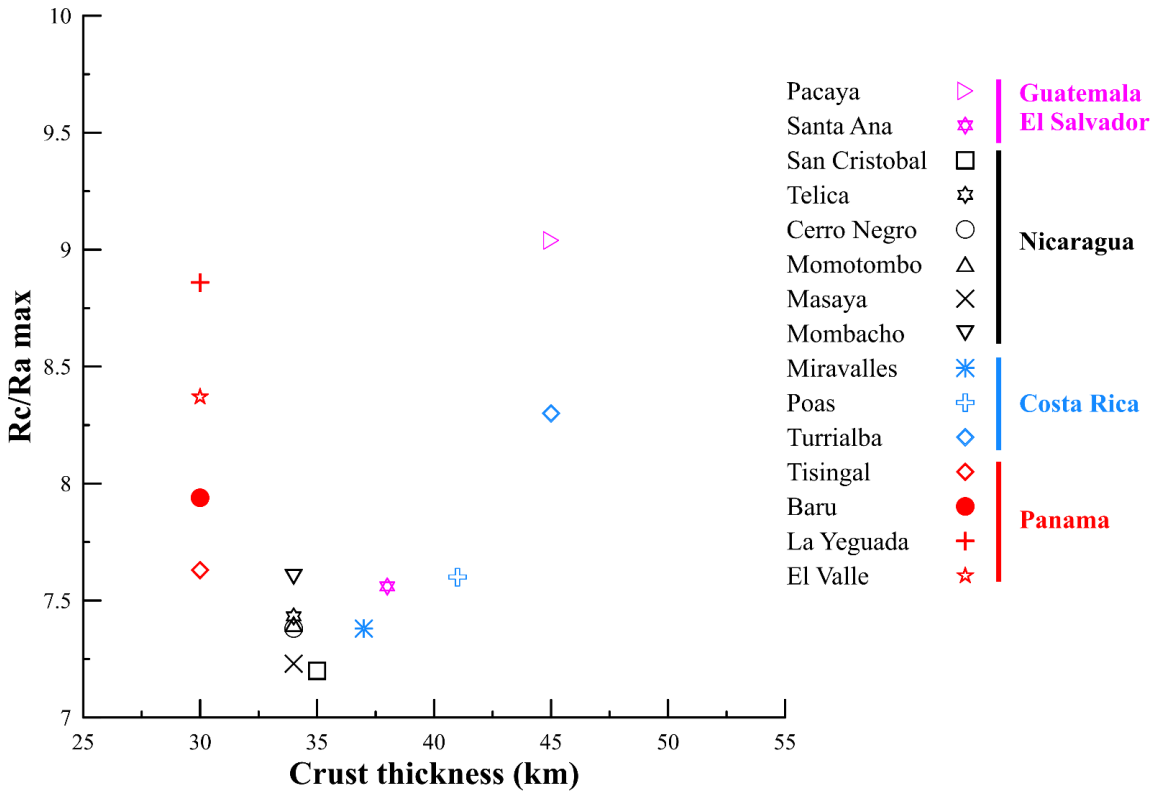

Figure 4. Crust thickness versus the maximum $^{3}He/^{4}He$ corrected for atmospheric contamination (Rc/Ra) measured in a selection of volcanoes from different segments of CAVA. Data selection is based on the criteria discussed in the text. Data source for the volcanoes, other than Telica and Baru, is reported in Figures 2 and 3 captions and in Tables S3 and S4. Crust thickness values below the selected volcanoes are from [16–19,106].

It must be recalled that the Panamanian volcanoes (Tisingal, Baru, La Yeguada and El Valle) are considered part of CAVA (Figure 1A), although the erupted rocks are of variable (and in part different) composition, and formed in a different geodynamic context with respect to the neighbouring Costarican segment. Two eruptive periods were identified for the Panamanian volcanoes: (1) from Miocene to about 5 Ma, during which rocks show typical calcalkaline features as in the rest of CAVA [110,112], and (2) Quaternary volcanism, starting after a ~2–3 Ma hiatus, and characterised by adakitic magma affinity [67] and a few high-Nb basalts [11,13]. The adakitic signature is characterised by a high Sr/Y and significant depletion in heavy rare earth elements, which is not present in older calcalkaline rocks, while it is observed in some active centers across southern Costa Rica (e.g., Turrialba) [3,4,11,67,113,116,120]. While there is consensus that the old calcalkaline magmatism of Panama resulted from the subduction of oceanic crust, with features similar to the rest of CAVA [11,108,110,121,122], different models have been proposed to explain the Quaternary adakite and high-Nb magmatism. After a relatively abrupt shift in subduction angle beneath Panama, which occurred during the late Miocene [121,122] period, there is evidence of an oblique subduction of the Nazca plate under the so-called Panama Block at a rate of ~40 mm/yr [6,13,108,110,123] (Figure 1A). This subduction is ongoing and is aseismic, probably due to a slab made by hot oceanic lithosphere [108]. What is controversial and strongly debated is the origin of the adakite and high-Nb magmatism in Quaternary volcanoes [26], and the role played by the paleo-Galápagos Hotspot track that lies >1500 m above the surrounding seafloor [124]. The most recurrent models invoke: (i) melting of the subducting oceanic crust of young (<25 Ma) age [3,4,10,11,67,108,113,114]; (ii) formation of a slab window that opened 8 Ma ago [115,116]; (iii) subduction erosion of the overlying plate [117]; (iv) high pressure crystal fractionation [13–15,114,118]; (v) formation of a slab

tear arising from subduction of the Panama Fracture Zone [119]; (vi) infiltration of Galapagos plume-like mantle "wind" through the hypothesised slab window [61] (Figure 1A).

We compare the available Rc/Ra signatures of CAVA volcanoes with their corresponding Ba/La and U/Th ratios in Figure 5. We find a systematic negative tendency, in which the lowest $^{3}He/^{4}He$ values in the Nicaraguan volcanoes are matched by the highest Ba/La and U/Th ratios; while the highest $^{3}He/^{4}He$ values are found associated with MORB-OIB-like [95], low Ba/La and U/Th ratios (in both Guatemala and Panama). This trend was first brought to light by [38,44] in their studies focussing on the Turrialba and San Cristobal volcanoes, respectively, and was interpreted as being due to a common slab fluid control on He and trace element signatures. Here, we provide additional validation and support to these ealier studies thanks to the availability of new $^{3}He/^{4}He$ results, especially for previously unstudied volcanoes from Nicaragua and Panama. We conclude from Figure 5 that slab fluids do play a central role in determining the mantle/magmatic $^{3}He/^{4}He$ signature at CAVA. If this interpretation is correct, then the distinct Telica vs. Baru signatures found here may simply result from a higher presence of subducted slab sediment fluids (rich in U and Th, from which radiogenic He is produced) in the Nicaraguan mantle wedge.

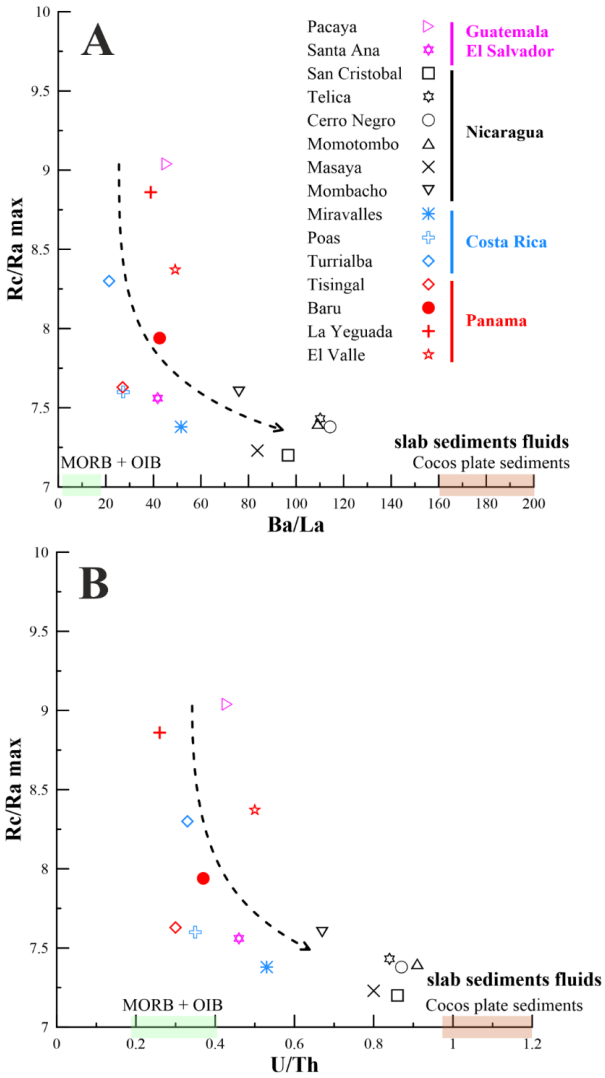

Figure 5. Ba/La (**A**) and U/Th (**B**) mean values (taken from GeoRoc pre-compiled files, considering only samples with SiO_2 < 60 wt.%; [125,126] versus the $^{3}He/^{4}He$ corrected for atmospheric contamination (Rc/Ra), for the selection of volcanoes from different segments of CAVA already mentioned in Figure 4 caption. Trace elements ratios for MORB, OIB and Cocos plate sediments are taken from [127–129].

Our conclusion of a dominant slab control on the He signature at Baru is not inconsistent with the results of Bekaert et al. (2021). The authors interpreted the highest $^{3}He/^{4}He$ (8.9 Ra), measured in a "cold" spring (T = 50 °C) from central Panama, as a mixture between crustal ^{4}He and a mantle source with $^{3}He/^{4}He$ as high as 10.3 Ra, and potentially up to 26 Ra. This higher than MORB $^{3}He/^{4}He$ signature would derive from the infiltration of Galapagos plume-like mantle "wind" through a slab window ([61]; Figure 1A). Geophysical and mantle flow modelling evidence suggests that the influx of Galapagos mantle plume materials would concentrate behind the volcanic front (where alkaline magmatism prevails); in contrast, adakitic volcanoes, such as Baru, would be located at the edge of the slab window, where magmatism would result from the partial melting of the subducting slab during the influx of hot astenosphere [61]. As such, a dominant slab control for Baru volcanism is implied in (and thus fully consistent with) the model of Bekaert et al. (2021).

With our results alone, we can neither support nor dismiss the hypothesis of a Galapagos mantle plume inflow in the Panama back-arc. We yet notice the mantle plume hypothesis [61] requires large (>14%, and up to 66%) He contribution from the crust, for which available CAVA results (Figures 4 and S2) bring little evidence. If crustal He addition was to be demonstrated marginal at CAVA, then the model of Bekaert et al. (2021) would need to be considered. At Pacaya volcano in Guatemala, for example, the measured $^{3}He/^{4}He$ ratios in FI [46] range 8.4-9.0 Ra, and yet no influx of Galapagos plume materials can be postulated or admitted from the rocks' geochemistry (Figures S2 and S3; e.g., [20]. Ultimately, it cannot be excluded that the ~9.0 Ra $^{3}He/^{4}He$ found in the cold spring of Panama reflects direct degassing of a MORB-type mantle (like below Pacaya), with very marginal (if any) crustal and slab additions.

We conclude that further multidisciplinary studies, and additional $^{3}He/^{4}He$ results (especially for alkaline volcanism behind the front), are required to deepen our knowledge on volatile sources underneath central Panama.

5. Conclusions

In arc volcanism, constraining the composition of noble gases is difficult, as they are prone to modifications starting in the wedge, due to the possible influence of subducting slabs, and potentially continuing in the overlying continental crust.

Here, we reported the first data of noble gases (He, Ne, Ar) for FI trapped in Ol and Px crystals from the Telica and Baru volcanoes, located in the Nicaraguan and Panamanian segments of CAVA, respectively. Previous studies reporting $^{3}He/^{4}He$ data for these volcanoes were limited to measurements in spring gases, which are known to be potentially prone to the addition of crustal He. The most important conclusions of the present study are:

- The magmatic air corrected $^{3}He/^{4}He$ signature for Telica and Baru is 7.5 Ra and 8.0 Ra, respectively, both within the MORB range (8 $\pm$ 1 Ra).
- A data quality check for our, and previous, $^{3}He/^{4}He$ measurements in FI, fumaroles and springs from the Nicaraguan and Panamanian arc segments, as well as for other CAVA volcanoes, brought to light an along-arc variability of the Rc/Ra signature. The lowest ratios are found in the Nicaraguan volcanoes, whereas $^{3}He/^{4}He$ ranges between 7.2 and 7.6 Ra with about 34–35 km of crust thickness. The Pacaya (Guatemala) and Turrialba (Costa Rica) volcanoes show the highest ratios with values up to 9.0 and 8.3 Ra, respectively, being both volcanoes built over about 45 km thick continental crust.
- The observed $^{3}He/^{4}He$ variability does not depend on the variable crust thickness reported for CAVA. Instead, it more likely reflects a contamination of the wedge by slab sediment fluids, which is marked in the Nicaraguan arc segment.

The $^{3}He/^{4}He$ signature of southern Costa Rica and the Baru volcano in western Panama seem to be influenced by change in subduction conditions, the possible presence of a slab window and the contemporary subduction of the Galapagos OIB-like hot-spot track.

Supplementary Materials: The following are available online at https://www.mdpi.com/article/10.3390/app12094241/s1, Figure S1: Mineral Chemistry—Diagram, Figure S2: Plots of Geomarker ratios vs. distance (km) along the arc from the border between NW and SE CAVA, Figure S2: Binary plots of Geomarker ratios, Figure S3: The trace and rare earth element data ratios are plotted in binary diagrams. Table S1: Bulk rock data composition, Table S2: Mineral chemistry, Table S3: Isotopic noble gas data from gases in CAVA literature, Table S4: Isotopic noble gas data from FIs in CAVA literature.

Author Contributions: Conceptualization, A.L.R., P.R. and A.D.P.; methodology, A.L.R. and P.R.; data curation, A.L.R. and P.R.; writing—original draft preparation, A.L.R. and P.R.; writing—review and editing, A.L.R., P.R., A.A. and A.D.P.; funding acquisition, A.L.R., P.R. and A.A. All authors have read and agreed to the published version of the manuscript.

Funding: This research was funded by the Italian Ministry of Education, Universities and Research (MIUR), grant number PRIN-2017LMNLAW and "The APC was funded by A.L.R. waiver by MDPI". This research was funded by (ANID) Fondecyt Iniciacion a la Investigacion de Philippe Robidoux, Etapa 2021, grant number N11190846. Field and sampling cost during 2015–2016 were covered by Universitá degli studi di Palermo (Italy)/Istituto Nazionale Previdenza Sociale INPS/Doctoral research scholarship for international students, and also by Fonds Québecois de Recherche Nature et technologies (FQRNT): Doctoral research scholarship (B2), 2013–2016.

Data Availability Statement: The Rutgers University Central American geochemical dataset "RU_CAGeochem" (DOI: 10.1002/gdj3.10) is consulted and represent database from the Geochemical Database by Carr et al. (2013) including Carr and Rose (1987) CENTAM database. The international databases EarthChem (http://www.earthchem.org/, accessed on 10 December 2021) and the Geochemistry of Rocks of the Oceans and Continents (GEOROC) (http://georoc.mpch-mainz.gwdg.de/georoc/Start.asp, accessed on 10 December 2021) were both consulted to access the geochemical datasets.

Acknowledgments: The Authors thank INGV, Sezione di Palermo, for providing the access to the noble gas isotopic laboratory. They are also grateful to Mariagrazia Misseri and Mariano Tantillo for technical support in the sample's preparation and noble gases analysis at INGV-Palermo. Piergiorgio Scarlato and Manuela Nazzari are also thanked for allowing access to the HPHT laboratory of INGV-Rome and providing technical support during electron microprobe analysis. The Authors appreciated the field and logistic support provided by Arkin Alaín Tapia-Espinosa and Eduardo Camacho A. The suggestions received by three anonymous Reviewers strongly improved the paper.

Conflicts of Interest: The authors declare no conflict of interest.

References

1. DeMets, C. A new estimate for present-day Cocos-Caribbean plate motion: Implications for slip along the Central American volcanic arc. *Geophys. Res. Lett.* **2001**, *28*, 4043–4046. [CrossRef]
2. O'Connor, J.M.; Stoffers, P.; Wijbrans, J.R.; Worthington, T.J. Migration of widespread long-lived volcanism across the Galápagos Volcanic Province: Evidence for a broad hotspot melting anomaly? *Earth Planet. Sci. Lett.* **2007**, *263*, 339–354. [CrossRef]
3. Gazel, E.; Carr, M.J.; Hoernle, K.; Feigenson, M.D.; Szymanski, D.; Hauff, F.; Van Den Bogaard, P. Galapagos-OIB signature in southern Central America: Mantle refertilization by arc–hot spot interaction. *Geochem. Geophys. Geosyst.* **2009**, *10*, 1–32. [CrossRef]
4. Gazel, E.; Hoernle, K.; Carr, M.J.; Herzberg, C.; Saginor, I.; Van den Bogaard, P.; Hauff, F.; Feigenson, M.; Swisher, C., III. Plume–subduction interaction in southern Central America: Mantle upwelling and slab melting. *Lithos* **2011**, *121*, 117–134. [CrossRef]
5. Chan, L.H.; Leeman, W.P.; You, C.F. Lithium isotopic composition of Central American volcanic arc lavas: Implications for modification of subarc mantle by slab-derived fluids: Correction. *Chem. Geol.* **2002**, *182*, 293–300. [CrossRef]
6. DeMets, C.; Gordon, R.G.; Argus, D.F. Geologically current plate motions. *Geophys. J. Int.* **2010**, *181*, 1–80. [CrossRef]
7. Protti, M.; Gu, F.; McNally, K. The geometry of the Wadati-Benioff zone under southern Central America and its tectonic significance: Results from a high-resolution local seismographic network. *Phys. Earth Planet. Inter.* **1994**, *84*, 271–287. [CrossRef]
8. Protti, M.; McNally, K.; Pacheco, J.; Gonzalez, V.; Montero, C.; Segura, J.; Brenes, J.; Barboza, V.; Malavassi, E.; Güendel, F.; et al. The March 25, 1990 (Mw = 7.0, ML = 6.8), earthquake at the entrance of the Nicoya Gulf, Costa Rica: Its prior activity, foreshocks, aftershocks, and triggered seismicity. *J. Geophys. Res. Solid Earth* **1995**, *100*, 20345–20358. [CrossRef]
9. Syracuse, E.M.; Abers, G.A. Global compilation of variations in slab depth beneath arc volcanoes and implications. *Geochem. Geophys. Geosyst.* **2006**, *7*, 1–18. [CrossRef]
10. De Boer, J.Z.; Drummond, M.S.; Bordelon, M.J.; Defant, M.J.; Bellon, H.; Maury, R.C. Early Tertiary arc volcanics from eastern Panama. In *Geologic and Tectonic Development of the Caribbean Plate Boundary in Southern Central America*; The Geological Society of America: Boulder, Colorado, 1995; Volume 295, pp. 35–56.

11. Defant, M.J.; Richerson, P.M.; De Boer, J.Z.; Stewart, R.H.; Maury, R.C.; Bellon, H.; Drummond, M.S.; Feigenson, M.D.; Jackson, T.E. Dacite genesis via both slab melting and differentiation: Petrogenesis of La Yeguada volcanic complex, Panama. *J. Petrol.* **1991**, *32*, 1101–1142. [CrossRef]
12. Sherrod, D.R.; Vallance, J.W.; Espinosa, A.T.; McGeehin, J.P. Volcán Barú—Eruptive history and volcano-hazards assessment. *US Geol. Surv. Open-File Rep.* **2007**, *2007*, 1401.
13. Hidalgo, P.J.; Rooney, T.O. Crystal fractionation processes at Baru volcano from the deep to shallow crust. *Geochem. Geophys. Geosyst.* **2010**, *11*, 1–29. [CrossRef]
14. Hidalgo, P.J.; Vogel, T.A.; Rooney, T.O.; Currier, R.M.; Layer, P.W. Origin of silicic volcanism in the Panamanian arc: Evidence for a two-stage fractionation process at El Valle volcano. *Contrib. Mineral. Petrol.* **2011**, *162*, 1115–1138. [CrossRef]
15. Hidalgo, P.J.; Rooney, T.O. Petrogenesis of a voluminous Quaternary adakitic volcano: The case of Baru volcano. *Contrib. Mineral. Petrol.* **2014**, *168*, 1–19. [CrossRef]
16. Carr, M.J. Symmetrical and segmented variation of physical and geochemical characteristics of the Central American volcanic front. *J. Volcanol. Geotherm. Res.* **1984**, *20*, 231–252. [CrossRef]
17. Abratis, M. Geochemical Variations in Magmatic Rocks from Southern Costa Rica as a Consequence of Cocos Ridge Subduction and Uplift of the Cordillera de Talamanca. Ph.D. Thesis, Georg-August-Universität Göttingen, Göttingen, Germany, 1998.
18. MacKenzie, L.; Abers, G.A.; Fischer, K.M.; Syracuse, E.M.; Protti, J.M.; Gonzalez, V.; Strauch, W. Crustal structure along the southern Central American volcanic front. *Geochem. Geophys. Geosyst.* **2008**, *9*, 1–19. [CrossRef]
19. Reguzzoni, M.; Sampietro, D. GEMMA: An Earth crustal model based on GOCE satellite data. *Int. J. Appl. Earth Obs. Geoinf.* **2015**, *35*, 31–43. [CrossRef]
20. Patino, L.C.; Carr, M.J.; Feigenson, M.D. Local and regional variations in Central American arc lavas controlled by variations in subducted sediment input. *Contrib. Mineral. Petrol.* **2000**, *138*, 265–283. [CrossRef]
21. Benjamin, E.R.; Plank, T.; Wade, J.A.; Kelley, K.A.; Hauri, E.H.; Alvarado, G.E. High water contents in basaltic magmas from Irazú Volcano, Costa Rica. *J. Volcanol. Geotherm. Res.* **2007**, *168*, 68–92. [CrossRef]
22. Hoernle, K.; Abt, D.L.; Fischer, K.M.; Nichols, H.; Hauff, F.; Abers, G.A.; Bogaard, P.V.D.; Heydolph, K.; Alvarado, G.; Protti, M.; et al. Arc-parallel flow in the mantle wedge beneath Costa Rica and Nicaragua. *Nature* **2008**, *451*, 1094–1097. [CrossRef]
23. Saginor, I.; Gazel, E.; Condie, C.; Carr, M.J. Evolution of geochemical variations along the Central American volcanic front. *Geochem. Geophys. Geosyst.* **2013**, *14*, 4504–4522. [CrossRef]
24. Walker, J.A.; Patino, L.C.; Carr, M.J.; Feigenson, M.D. Slab control over HFSE depletions in central Nicaragua. *Earth Planet. Sci. Lett.* **2001**, *192*, 533–543. [CrossRef]
25. Sadofsky, S.J.; Portnyagin, M.; Hoernle, K.; van den Bogaard, P. Subduction cycling of volatiles and trace elements through the Central American volcanic arc: Evidence from melt inclusions. *Contrib. Mineral. Petrol.* **2008**, *155*, 433–456. [CrossRef]
26. Rooney, T.O.; Morell, K.D.; Hidalgo, P.; Fraceschi, P. Magmatic consequences of the transition from orthogonal to oblique subduction in P anama. *Geochem. Geophys. Geosyst.* **2015**, *16*, 4178–4208. [CrossRef]
27. Sano, Y.; Williams, S.N. Fluxes of mantle and subducted carbon along convergent plate boundaries. *Geophys. Res. Lett.* **1996**, *23*, 2749–2752. [CrossRef]
28. Tassi, F.; Vaselli, O.; Barboza, V.; Fernandez, E.; Duarte, E. Fluid geochemistry and seismic activity in the period 1998–2002 at Turrialba Volcano (Costa Rica). *Ann. Geophysics* **2004**, *47*, 1501–1511.
29. Hilton, D.R.; Ramirez, C.J.; Mora-Amador, R.; Fischer, T.P.; Füri, E.; Barry, P.H.; Shaw, A.M. Monitoring of temporal and spatial variations in fumarole helium and carbon dioxide characteristics at Poás and Turrialba volcanoes, Costa Rica (2001–2009). *Geochem. J.* **2010**, *44*, 431–440. [CrossRef]
30. Vaselli, O.; Tassi, F.; Duarte, E.; Fernandez, E.; Poreda, R.J.; Huertas, A.D. Evolution of fluid geochemistry at the Turrialba volcano (Costa Rica) from 1998 to 2008. *Bull. Volcanol.* **2010**, *72*, 397–410. [CrossRef]
31. Aiuppa, A.; Robidoux, P.; Tamburello, G.; Conde, V.; Galle, B.; Avard, G.; Bagnato, E.; De Moor, J.M.; Martínez, M.; Muñoz, A. Gas measurements from the Costa Rica–Nicaragua volcanic segment suggest possible along-arc variations in volcanic gas chemistry. *Earth Planet. Sci. Lett.* **2014**, *407*, 134–147. [CrossRef]
32. Aiuppa, A.; Bitetto, M.; Francofonte, V.; Velasquez, G.; Parra, C.B.; Giudice, G.; Liuzzo, M.; Moretti, R.; Moussallam, Y.; Peters, N.; et al. A CO_2-gas precursor to the March 2015 Villarrica volcano eruption. *Geochem. Geophys. Geosyst.* **2017**, *18*, 2120–2132. [CrossRef]
33. Conde, V.; Bredemeyer, S.; Duarte, E.; Pacheco, J.F.; Miranda, S.; Galle, B.; Hansteen, T.H. SO_2 degassing from Turrialba Volcano linked to seismic signatures during the period 2008–2012. *Int. J. Earth Sci.* **2014**, *103*, 1983–1998. [CrossRef]
34. Fischer, T.P.; Ramírez, C.; Mora-Amador, R.A.; Hilton, D.R.; Barnes, J.D.; Sharp, Z.D.; Brun, M.L.; de Moor, J.M.; Barry, P.H.; Füri, E.; et al. Temporal variations in fumarole gas chemistry at Poás volcano, Costa Rica. *J. Volcanol. Geotherm. Res.* **2015**, *294*, 56–70. [CrossRef]
35. De Moor, J.M.; Aiuppa, A.; Avard, G.; Wehrmann, H.; Dunbar, N.; Muller, C.; Tamburello, G.; Giudice, G.; Liuzzo, M.; Moretti, R.; et al. Turmoil at Turrialba Volcano (Costa Rica): Degassing and eruptive processes inferred from high-frequency gas monitoring. *J. Geophys. Res. Solid Earth* **2016**, *121*, 5761–5775. [CrossRef] [PubMed]

36. De Moor, J.M.; Kern, C.; Avard, G.; Muller, C.; Aiuppa, A.; Saballos, A.; Ibarra, M.; LaFemina, P.; Protti, M.; Fischer, T.P. A new sulfur and carbon degassing inventory for the Southern Central American Volcanic Arc: The importance of accurate time-series data sets and possible tectonic processes responsible for temporal variations in arc-scale volatile emissions. *Geochem. Geophys. Geosyst.* **2017**, *18*, 4437–4468. [CrossRef]
37. Moussallam, Y.; Peters, N.; Ramirez, C.; Oppenheimer, C.; Aiuppa, A.; Giudice, G. Characterisation of the magmatic signature in gas emissions from Turrialba Volcano, Costa Rica. *Solid Earth* **2014**, *5*, 1341–1350. [CrossRef]
38. Di Piazza, A.; Rizzo, A.L.; Barberi, F.; Carapezza, M.L.; De Astis, G.; Romano, C.; Sortino, F. Geochemistry of the mantle source and magma feeding system beneath Turrialba volcano, Costa Rica. *Lithos* **2015**, *232*, 319–335. [CrossRef]
39. Rizzo, A.L.; Di Piazza, A.; de Moor, J.M.; Alvarado, G.E.; Avard, G.; Carapezza, M.L.; Mora, M.M. Eruptive activity at Turrialba volcano (Costa Rica): Inferences from 3 He/4 He in fumarole gases and chemistry of the products ejected during 2014 and 2015. *Geochem. Geophys. Geosyst.* **2016**, *17*, 4478–4494. [CrossRef]
40. Allard, P. The origin of hydrogen, carbon, sulfur, nitrogen, and rare gases in volcanic exhalations: Evidence from isotope geochemistry. In *Forecasting Volcanic Events*; Tazieff, H., Sabroux, J.-C., Eds.; Elsevier: Amsterdam, The Netherlands, 1983; pp. 337–386.
41. Burton, M.R.; Oppenheimer, C.; Horrocks, L.A.; Francis, P.W. Remote sensing of CO_2 and H_2O emission rates from Masaya volcano, Nicaragua. *Geology* **2000**, *28*, 915–918. [CrossRef]
42. Shaw, A.M.; Hilton, D.R.; Fischer, T.P.; Walker, J.A.; Alvarado, G.E. Contrasting He–C relationships in Nicaragua and Costa Rica: Insights into C cycling through subduction zones. *Earth Planet. Sci. Lett.* **2003**, *214*, 499–513. [CrossRef]
43. Martin, R.S.; Sawyer, G.M.; Spampinato, L.; Salerno, G.G.; Ramirez, C.; Ilyinskaya, E.; Witt, M.L.I.; Mather, T.A.; Watson, I.M.; Phillips, J.C.; et al. A total volatile inventory for Masaya Volcano, Nicaragua. *J. Geophys. Res. Solid Earth* **2010**, *115*, 1–12. [CrossRef]
44. Robidoux, P.; Aiuppa, A.; Rotolo, S.G.; Rizzo, A.L.; Hauri, E.H.; Frezzotti, M.L. Volatile contents of mafic-to-intermediate magmas at San Cristóbal volcano in Nicaragua. *Lithos* **2017**, *272*, 147–163. [CrossRef]
45. Goff, F.; McMurtry, G.M. Tritium and stable isotopes of magmatic waters. *J. Volcanol. Geotherm. Res.* **2000**, *97*, 347–396. [CrossRef]
46. Battaglia, A.; Bitetto, M.; Aiuppa, A.; Rizzo, A.L.; Chigna, G.; Watson, I.M.; D'Aleo, R.; Juárez Cacao, F.J.; de Moor, M.J. The Magmatic gas Signature of Pacaya Volcano, with implications for the volcanic CO2 flux from Guatemala. *Geochem. Geophys. Geosyst.* **2018**, *19*, 667–692. [CrossRef]
47. Martelli, M.; Rizzo, A.L.; Renzulli, A.; Ridolfi, F.; Arienzo, I.; Rosciglione, A. Noble-gas signature of magmas from a heterogeneous mantle wedge: The case of Stromboli volcano (Aeolian Islands, Italy). *Chem. Geol.* **2014**, *368*, 39–53. [CrossRef]
48. Barry, P.H.; Nakagawa, M.; Giovannelli, D.; Maarten de Moor, J.; Schrenk, M.; Seltzer, A.M.; Manini, E.; Fattorini, D.; di Carlo, M.; Regoli, F.; et al. Helium, inorganic and organic carbon isotopes of fluids and gases across the Costa Rica convergent margin. *Sci. Data* **2019**, *6*, 1–8. [CrossRef] [PubMed]
49. Rizzo, A.; Barberi, F.; Carapezza, M.L.; Di Piazza, A.; Francalanci, L.; Sortino, F.; D'Alessandro, W. New mafic magma refilling a quiescent volcano: Evidence from He–Ne–Ar isotopes during the 2011–2012 unrest at Santorini, Greece. *Geochem. Geophys. Geosyst.* **2015**, *16*, 798–814. [CrossRef]
50. Rizzo, A.L.; Caracausi, A.; Chavagnac, V.; Nomikou, P.; Polymenakou, P.N.; Mandalakis, M.; Kotoulas, G.; Magoulas, A.; Castillo, A.; Lampridou, D. Kolumbo submarine volcano (Greece): An active window into the Aegean subduction system. *Sci. Rep.* **2016**, *6*, 1–9. [CrossRef]
51. Rizzo, A.L.; Caracausi, A.; Chavagnac, V.; Nomikou, P.; Polymenakou, P.; Mandalakis, M.; Kotoulas, G.; Magoulas, A.; Castillo, A.; Lampridou, D.; et al. Geochemistry of CO_2-rich gases venting from submarine volcanism: The case of Kolumbo (Hellenic Volcanic Arc, Greece). *Front. Earth Sci.* **2019**, *7*, 1–20. [CrossRef]
52. Lages, J.; Rizzo, A.L.; Aiuppa, A.; Robidoux, P.; Aguilar, R.; Apaza, F.; Masias, P. Crustal controls on light noble gas isotope variability along the Andean Volcanic Arc. *Geochem. Perspect. Lett.* **2021**, *19*, 45–49. [CrossRef]
53. Lages, J.; Rizzo, A.L.; Aiuppa, A.; Samaniego, P.; Le Pennec, J.L.; Ceballos, J.A.; Narvaez, P.A.; Moussallam, Y.; Bani, P.; Schipper, C.I.; et al. Noble gas magmatic signature of the Andean Northern Volcanic Zone from fluid inclusions in minerals. *Chem. Geol.* **2021**, *559*, 119966. [CrossRef]
54. Poreda, R.; Craig, H. Helium isotope ratios in circum-Pacific volcanic arcs. *Nature* **1989**, *338*, 473–478. [CrossRef]
55. Janik, C.J.; Goff, F.; Fahlquist, L.; Adams, A.I.; Roldan, M.A.; Chipera, S.J.; Trujillo, P.E.; Counce, D. Hydrogeochemical exploration of geothermal prospects in the Tecuamburro volcano region, Guatemala. *Geothermics* **1992**, *21*, 447–481. [CrossRef]
56. Snyder, G.; Poreda, R.; Hunt, A.; Fehn, U. Regional variations in volatile composition: Isotopic evidence for carbonate recycling in the Central American volcanic arc. *Geochem. Geophys. Geosyst.* **2001**, *2*, 1–25. [CrossRef]
57. Snyder, G.; Poreda, R.; Fehn, U.; Hunt, A. Sources of nitrogen and methane in Central American geothermal settings: Noble gas and 129I evidence for crustal and magmatic volatile components. *Geochem. Geophys. Geosyst.* **2003**, *4*, 1–28. [CrossRef]
58. Elkins, L.J.; Fischer, T.P.; Hilton, D.R.; Sharp, Z.D.; McKnight, S.; Walker, J. Tracing nitrogen in volcanic and geothermal volatiles from the Nicaraguan volcanic front. *Geochim. Et Cosmochim. Acta* **2006**, *70*, 5215–5235. [CrossRef]
59. De Leeuw, G.A.M.; Hilton, D.R.; Fischer, T.P.; Walker, J.A. The He–CO_2 isotope and relative abundance characteristics of geothermal fluids in el salvador and honduras: New constraints on volatile mass balance of the central american volcanic arc. *Earth Planet. Sci. Lett.* **2007**, *258*, 132–146. [CrossRef]
60. Lucic, G.; Stix, J.; Sherwood Lollar, B.; Lacrampe-Couloume, G.; Muñoz, A.; Carcache, M.I. The degassing character of a young volcanic center: Cerro Negro, Nicaragua. *Bull. Volcanol.* **2014**, *76*, 1–23. [CrossRef]

61. Bekaert, D.V.; Gazel, E.; Turner, S.; Behn, M.D.; De Moor, J.M.; Zahirovic, S.; Manea, V.C.; Hoernle, K.; Fischer, T.P.; Hammerstrom, A.; et al. High 3He/4He in central Panama reveals a distal connection to the Galápagos plume. *Proc. Natl. Acad. Sci. USA* **2021**, *118*, e2110997118. [CrossRef]
62. Fischer, T.P.; Marty, B. Volatile abundances in the sub-arc mantle: Insights from volcanic and hydrothermal gas discharges. *J. Volcanol. Geotherm. Res.* **2005**, *140*, 205–216. [CrossRef]
63. Shaw, A.M.; Hilton, D.R.; Fischer, T.P.; Walker, J.A.; De Leeuw, G.A.M. Helium isotope variations in mineral separates from Costa Rica and Nicaragua: Assessing crustal contributions, timescale variations and diffusion-related mechanisms. *Chem. Geol.* **2006**, *230*, 124–139. [CrossRef]
64. Conde, V.; Nilsson, D.; Galle, B.; Cartagena, R.; Muñoz, A. A rapid deployment instrument network for temporarily monitoring volcanic SO_2 emissions—A case study from Telica volcano. *Geosci. Instrum. Methods Data Syst.* **2014**, *3*, 127–134. [CrossRef]
65. Rodgers, M.; Roman, D.C.; Geirsson, H.; LaFemina, P.; Muñoz, A.; Guzman, C.; Tenorio, V. Seismicity accompanying the 1999 eruptive episode at Telica Volcano, Nicaragua. *J. Volcanol. Geotherm. Res.* **2013**, *265*, 39–51. [CrossRef]
66. Defant, M.J.; Drummond, M.S. Derivation of some modern arc magmas by melting of young subducted lithosphere. *Nature* **1990**, *347*, 662–665. [CrossRef]
67. Maury, R.C.; Defant, M.J.; Belon, H.; de Boer, J.Z.; Stewart, R.W.; Cotten, J. Early Tertiary arc volcanics from eastern Panama. In *Geologic and Tectonic Development of the Caribbean Plate Boundary in Southern Central America: Geological Society of America Special Paper*; Mann, P., Ed.; The Geological Society of America: Boulder, Colorado, 1995; Volume 295, pp. 29–34.
68. Wegner, W.; Wörner, G.; Harmon, R.S.; Jicha, B.R. Magmatic history and evolution of the Central American Land Bridge in Panama since Cretaceous times. *Bulletin* **2011**, *123*, 703–724. [CrossRef]
69. Kurz, M.D. Cosmogenic helium in a terrestrial igneous rock. *Nature* **1986**, *320*, 435–439. [CrossRef]
70. Hilton, D.R.; Hammerschmidt, K.; Teufel, S.; Friedrichsen, H. Helium isotope characteristics of Andean geothermal fluids and lavas. *Earth Planet. Sci. Lett.* **1993**, *120*, 265–282. [CrossRef]
71. Hilton, D.R.; Fischer, T.P.; Marty, B. Noble gases and volatile recycling at subduction zones. *Rev. Mineral. Geochem.* **2002**, *47*, 319–370. [CrossRef]
72. Robidoux, P.; Rotolo, S.G.; Aiuppa, A.; Lanzo, G.; Hauri, E.H. Geochemistry and volatile content of magmas feeding explosive eruptions at Telica volcano (Nicaragua). *J. Volcanol. Geotherm. Res.* **2017**, *341*, 131–148. [CrossRef]
73. Havlicek, P.; Hradecky, P.; Hrubes, M.; Mlcoch, B.; Opletal, M.; Sebesta, J.; Buitrago, N.; Strauch, W. *Estudio Geológico Y Reconocimiento De La Amenaza Natural—Zona Chinandega-Leon, Nicaragua. Praga-Managua 1999, Resumen Ejecutivo (Servicio Geológico Checo, CGU, en Cooperación con Instituto Nicaragüense de Estudios Territoriales, INETER)*; CGU: Pragua, Czech, 1999; 23p.
74. Havlicek, P.; Hradecky, P.; Hrubes, M.; Kyel, P.; Mlcoch, B.; Mrazova, S.; Novak, Z.; Opletal, M.; Prichystal, A.; Sebesta, J.; et al. *Estudio Geológico Y Reconocimiento De La Amenaza Geológica En El Área De León—La Paz Centro Y Malpasillo, Praga-Managua 2000, Reporte Final (Servicio Geológico Checo, CGU, en Cooperación con Instituto Nicaragüense de Estudios Territoriales, INETER)*; CGU: Pragua, Czech, 2000; 244p.
75. McClelland, L. (Ed.) Global Volcanism Program. Report on Telica (Nicaragua). In *Scientific Event Alert Network Bulletin, 7:2. Smithsonian Institution*; Smithsonian Institution: Washington, DC, USA, 1982. [CrossRef]
76. Robidoux, P.; Rizzo, A.L.; Aguilera, F.; Aiuppa, A.; Artale, M.; Liuzzo, M.; Nazzari, M.; Zummo, F. Petrological and noble gas features of Lascar and Lastarria volcanoes (Chile): Inferences on plumbing systems and mantle characteristics. *Lithos* **2020**, *370*, 105615. [CrossRef]
77. Robidoux, P.; Pastén, D.; Levresse, G.; Diaz, G.; Paredes, D. Volatile Content Implications of Increasing Explosivity of the Strombolian Eruptive Style along the Fracture Opening on the NE Villarrica Flank: Minor Eruptive Centers in the Los Nevados Group 2. *Geosciences* **2021**, *11*, 309. [CrossRef]
78. Rizzo, A.L.; Pelorosso, B.; Coltorti, M.; Ntaflos, T.; Bonadiman, C.; Matusiak-Małek, M.; Italiano, F.; Bergonzoni, G. Geochemistry of noble gases and CO_2 in fluid inclusions from lithospheric mantle beneath Wilcza Góra (Lower Silesia, southwest Poland). *Front. Earth Sci.* **2018**, *6*, 215. [CrossRef]
79. Rizzo, A.L.; Faccini, B.; Casetta, F.; Faccincani, L.; Ntaflos, T.; Italiano, F.; Coltorti, M. Melting and metasomatism in West Eifel and Siebengebirge Sub-Continental Lithospheric Mantle: Evidence from concentrations of volatiles in fluid inclusions and petrology of ultramafic xenoliths. *Chem. Geol.* **2021**, *581*, 120400. [CrossRef]
80. Sano, Y.; Wakita, H. Geographical distribution of 3He/4He ratios in Japan: Implications for arc tectonics and incipient magmatism. *J. Geophys. Res. Solid Earth* **1985**, *90*, 8729–8741. [CrossRef]
81. Carr, M.J.; Rose, W.I., Jr. CENTAM—a data base of Central American volcanic rocks. *J. Volcanol. Geotherm. Res.* **1987**, *33*, 239–240. [CrossRef]
82. Heydolph, K.; Hoernle, K.; Hauff, F.; van den Bogaard, P.; Portnyagin, M.; Bindeman, I.; Garbe-Schönberg, D. Along and across arc geochemical variations in NW Central America: Evidence for involvement of lithospheric pyroxenite. *Geochim. Cosmochim. Acta* **2012**, *84*, 459–491. [CrossRef]
83. Gale, A.; Dalton, C.A.; Langmuir, C.H.; Su, Y.; Schilling, J.G. The mean composition of ocean ridge basalts. *Geochem. Geophys. Geosyst.* **2013**, *14*, 489–518. [CrossRef]
84. Ozima, M.; Podosek, F.A. *Noble Gas Geochemistry*; Cambridge University Press: Cambridge, UK, 2002.
85. Marty, B. The origins and concentrations of water, carbon, nitrogen and noble gases on Earth. *Earth Planet. Sci. Lett.* **2012**, *313*, 56–66. [CrossRef]

86. Nuccio, P.M.; Paonita, A.; Rizzo, A.; Rosciglione, A. Elemental and isotope covariation of noble gases in mineral phases from Etnean volcanics erupted during 2001–2005, and genetic relation with peripheral gas discharges. *Earth Planet. Sci. Lett.* **2008**, *272*, 683–690. [CrossRef]
87. Graham, D.W. Noble gas isotope geochemistry of mid-ocean ridge and ocean island basalts: Characterization of mantle source reservoirs. *Rev. Miner. Geochem.* **2002**, *47*, 247–319. [CrossRef]
88. Matsumoto, T.; Chen, Y.; Matsuda, J.I. Concomitant occurrence of primordial and recycled noble gases in the Earth's mantle. *Earth Planet. Sci. Lett.* **2001**, *185*, 35–47. [CrossRef]
89. Hopp, J.; Ionov, D.A. Tracing partial melting and subduction-related metasomatism in the Kamchatkan mantle wedge using noble gas compositions. *Earth Planet. Sci. Lett.* **2011**, *302*, 121–131. [CrossRef]
90. Hopp, J.; Trieloff, M.; Altherr, R. Noble gas compositions of the lithospheric mantle below the Chyulu Hills volcanic field, Kenya. *Earth Planet. Sci. Lett.* **2007**, *261*, 635–648. [CrossRef]
91. Yamamoto, J.; Kaneoka, I.; Nakai, S.I.; Kagi, H.; Prikhod'ko, V.S.; Arai, S. Evidence for subduction-related components in the subcontinental mantle from low 3He/4He and 40Ar/36Ar ratio in mantle xenoliths from Far Eastern Russia. *Chem. Geol.* **2004**, *207*, 237–259. [CrossRef]
92. Yamamoto, J.; Kagi, H.; Kawakami, Y.; Hirano, N.; Nakamura, M. Paleo-Moho depth determined from the pressure of CO2 fluid inclusions: Raman spectroscopic barometry of mantle-and crust-derived rocks. *Earth Planet. Sci. Lett.* **2007**, *253*, 369–377. [CrossRef]
93. Sandoval-Velasquez, A.; Rizzo, A.L.; Aiuppa, A.; Remigi, S.; Padron, E.; Perez, N.M.; Frezzotti, M.L. Recycled crustal carbon in the depleted mantle source of El Hierro volcano, Canary Islands. *Lithos* **2021**, *400*, 106414. [CrossRef]
94. Sandoval-Velasquez, A.; Rizzo, A.L.; Frezzotti, M.L.; Saucedo, R.; Aiuppa, A. The composition of fluids stored in the central Mexican lithospheric mantle: Inferences from noble gases and CO_2 in mantle xenoliths. *Chem. Geol.* **2021**, *576*, 120270. [CrossRef]
95. Hilton, D.R.; Barling, J.; Wheller, G.E. Effect of shallow-level contamination on the helium isotope systematics of ocean-island lavas. *Nature* **1995**, *373*, 330–333. [CrossRef]
96. Ballentine, C.J.; Burnard, P.G. Production, release and transport of noble gases in the continental crust. *Rev. Mineral. Geochem.* **2002**, *47*, 481–538. [CrossRef]
97. Paonita, A.; Caracausi, A.; Iacono-Marziano, G.; Martelli, M.; Rizzo, A. Geochemical evidence for mixing between fluids exsolved at different depths in the magmatic system of Mt Etna (Italy). *Geochim. Et Cosmochim. Acta* **2012**, *84*, 380–394. [CrossRef]
98. Caracausi, A.; Paternoster, M. Radiogenic helium degassing and rock fracturing: A case study of the southern Apennines active tectonic region. *J. Geophys. Res. Solid Earth* **2015**, *120*, 2200–2211. [CrossRef]
99. Boudoire, G.; Rizzo, A.L.; Arienzo, I.; Di Muro, A. Paroxysmal eruptions tracked by variations of helium isotopes: Inferences from Piton de la Fournaise (La Réunion island). *Sci. Rep.* **2020**, *10*, 1–16. [CrossRef] [PubMed]
100. Montoya-Lopera, P.; Levresse, G.; Ferrari, L.; Rizzo, A.L.; Urquiza, S.; Mata, L. Genesis of the telescoped Eocene silver and Oligocene gold San Dimas deposits, Sierra Madre Occidental, Mexico: Constraints from fluid inclusions, oxygen-deuterium and noble gases isotopes. *Ore Geol. Rev.* **2020**, *120*, 103427. [CrossRef]
101. Staudacher, T.; Allègre, C.J. Recycling of oceanic crust and sediments: The noble gas subduction barrier. *Earth Planet. Sci. Lett.* **1988**, *89*, 173–183. [CrossRef]
102. Sano, Y.; Fischer, T.P. The analysis and interpretation of noble gases in modern hydrothermal systems. In *The Noble Gases as Geochemical Tracers*; Springer: Berlin/Heidelberg, Germany, 2013; pp. 249–317.
103. Oppenheimer, C.; Fischer, T.P.; Scaillet, B. Volcanic degassing: Process and impact. *Treatise Geochem.* **2014**, *4*, 111–179.
104. Mason, E.; Edmonds, M.; Turchyn, A.V. Remobilization of crustal carbon may dominate volcanic arc emissions. *Science* **2017**, *357*, 290–294. [CrossRef]
105. Martelli, M.; Nuccio, P.M.; Stuart, F.M.; Burgess, R.; Ellam, R.M.; Italiano, F. Helium–strontium isotope constraints on mantle evolution beneath the Roman Comagmatic Province, Italy. *Earth Planet. Sci. Lett.* **2004**, *224*, 295–308. [CrossRef]
106. Case, J.E.; MacDonald, W.D.; Fox, P.J. Caribbean crustal provinces; seismic and gravidy evidence. In *The Caribbean Region*; Dengo, G., Case, J.E., Eds.; The Geology of North America: Boulder, NV, USA, 1990; pp. 15–36.
107. Carr, M.J.; Feigenson, M.D.; Bennett, E.A. Incompatible element and isotopic evidence for tectonic control of source mixing and melt extraction along the Central American arc. *Contrib. Mineral. Petrol.* **1990**, *105*, 369–380. [CrossRef]
108. De Boer, J.Z.; Defant, M.J.; Stewart, R.H.; Restrepo, J.F.; Clark, L.F.; Ramirez, A.H. Quaternary calc-alkaline volcanism in western Panama: Regional variation and implication for the plate tectonic framework. *J. S. Am. Earth Sci.* **1988**, *1*, 275–293. [CrossRef]
109. Defant, M.J.; Jackson, T.E.; Drummond, M.D.; De Boer, J.Z.; Bellon, H.; Feigenson, M.D.; Maury, R.C.; Stewart, R.H. The geochemistry of young volcanism throughout western Panama and southeastern Costa Rica: An overview. *J. Geol. Soc.* **1992**, *149*, 569–579. [CrossRef]
110. De Boer, J.Z.; Defant, M.J.; Stewart, R.H.; Bellon, H. Evidence for active subduction below western Panama. *Geology* **1991**, *19*, 649–652. [CrossRef]
111. Drummond, M.S.; Defant, M.J. A model for trondhjemite-tonalite-dacite genesis and crustal growth via slab melting: Archean to modern comparisons. *J. Geophys. Res. Solid Earth* **1990**, *95*, 21503–21521. [CrossRef]
112. Drummond, M.S.; Defant, M.J.; Kepezhinskas, P.K. Petrogenesis of slab-derived trondhjemite–tonalite–dacite/adakite magmas. *Earth Environ. Sci. Trans. R. Soc. Edinb.* **1996**, *87*, 205–215.

113. Drummond, M.S.; Bordelon, M.; De Boer, J.Z.; Defant, M.J.; Bellon, H.; Feigenson, M.D. Igneous petrogenesis and tectonic setting of plutonic and volcanic rocks of the Cordillera de Talamanca, Costa Rica-Panama, Central American arc. *Am. J. Sci.* **1995**, *295*, 875–919. [CrossRef]
114. Ribeiro, J.M.; Maury, R.C.; Grégoire, M. Are adakites slab melts or high-pressure fractionated mantle melts? *J. Petrol.* **2016**, *57*, 839–862. [CrossRef]
115. Johnston, S.T.; Thorkelson, D.J. Cocos-Nazca slab window beneath central America. *Earth Planet. Sci. Lett.* **1997**, *146*, 465–474. [CrossRef]
116. Abratis, M.; Wörner, G. Ridge collision, slab-window formation, and the flux of Pacific asthenosphere into the Caribbean realm. *Geology* **2001**, *29*, 127–130. [CrossRef]
117. Goss, A.R.; Kay, S.M. Steep REE patterns and enriched Pb isotopes in southern Central American arc magmas: Evidence for forearc subduction erosion? *Geochem. Geophys. Geosyst.* **2006**, *7*, 1–20. [CrossRef]
118. Rooney, T.O.; Franceschi, P.; Hall, C.M. Water-saturated magmas in the Panama Canal region: A precursor to adakite-like magma generation? *Contrib. Mineral. Petrol.* **2011**, *161*, 373–388. [CrossRef]
119. Morell, K.D.; Gardner, T.W.; Fisher, D.M.; Idleman, B.D.; Zellner, H.M. Active thrusting, landscape evolution, and late Pleistocene sector collapse of Barú Volcano above the Cocos-Nazca slab tear, southern Central America. *Bulletin* **2013**, *125*, 1301–1318. [CrossRef]
120. Gazel, E.; Hayes, J.L.; Hoernle, K.; Kelemen, P.; Everson, E.; Holbrook, W.S.; Hauff, F.; Van Den Bogaard, P.; Vance, E.A.; Chu, S.; et al. Continental crust generated in oceanic arcs. *Nat. Geosci.* **2015**, *8*, 321–327. [CrossRef]
121. Morell, K.D. Late M iocene to recent plate tectonic history of the southern C entral A merica convergent margin. *Geochem. Geophys. Geosyst.* **2015**, *16*, 3362–3382. [CrossRef]
122. Morell, K.D.; Kirby, E.; Fisher, D.M.; van Soest, M. Geomorphic and exhumational response of the Central American Volcanic Arc to Cocos Ridge subduction. *J. Geophys. Res. Solid Earth* **2012**, *117*, 1–23. [CrossRef]
123. Trenkamp, R.; Kellogg, J.N.; Freymueller, J.T.; Mora, H.P. Wide plate margin deformation, southern Central America and northwestern South America, CASA GPS observations. *J. S. Am. Earth Sci.* **2002**, *15*, 157–171. [CrossRef]
124. Walther, C.H. The crustal structure of the Cocos ridge off Costa Rica. *J. Geophys. Res. Solid Earth* **2003**, *108*, 1–21. [CrossRef]
125. Geochemistry of Rocks of the Oceans and Continents (GEOROC). Available online: http://georoc.mpch-mainz.gwdg.de/georoc/ (accessed on 10 December 2021).
126. EarthChem. Available online: http://www.earthchem.org/ (accessed on 10 December 2021).
127. Hofmann, A.W. Chemical differentiation of the Earth: The relationship between mantle, continental crust, and oceanic crust. *Earth Planet. Sci. Lett.* **1988**, *90*, 297–314. [CrossRef]
128. Sun, S.S.; McDonough, W.F. Chemical and isotopic systematics of oceanic basalts: Implications for mantle composition and processes. *Geol. Soc. Lond. Spec. Publ.* **1989**, *42*, 313–345. [CrossRef]
129. Plank, T.; Langmuir, C.H. The chemical composition of subducting sediment and its consequences for the crust and mantle. *Chem. Geol.* **1998**, *145*, 325–394. [CrossRef]